2-24-2012

Evolution of the Earliest Horses Driven by Climate Change in the Paleocene-Eocene Thermal Maximum

Ross Secord
University of Nebraska-Lincoln, rsecord2@unl.edu

Jonathan I. Bloch
Florida Museum of Natural History, University of Florida, jbloch@flmnh.ufl.edu

Stephen G. B. Chester
Yale University, stephen.chester@yale.edu

Doug M. Boyer
Brooklyn College, City University of New York, douglasmb@gmail.com

Aaron R. Wood
South Dakota School of Mines and Technology, Aaron.Wood@sdsmt.edu

See next page for additional authors

Published in *Science* vol. 335 no. 6071 (February 24, 2012), pp. 959-962; doi: 10.1126/science.1213859

Submitted September 12, 2011; accepted January 13, 2012.

Evolution of the Earliest Horses Driven by Climate Change in the Paleocene-Eocene Thermal Maximum

Ross Secord,[1,2] Jonathan I. Bloch,[2], Stephen G. B. Chester,[3] Doug M. Boyer,[4] Aaron R. Wood,[5,2] Scott L. Wing,[6] Mary J. Kraus,[7] Francesca A. McInerney,[8] John Krigbaum,[9]

1. Department of Earth and Atmospheric Sciences, University of Nebraska, Lincoln, NE 68588, USA
2. Florida Museum of Natural History, University of Florida, Gainesville, FL 32611–7800, USA
3. Department of Anthropology, Yale University, New Haven, CT, 06520, USA
4. Department of Anthropology and Archaeology, Brooklyn College, City University of New York, New York, NY 11210, USA
5. Department of Geology and Geological Engineering, South Dakota School of Mines and Technology, Rapid City, SD 57701, USA
6. Department of Paleobiology, Smithsonian Museum of Natural History, Washington, DC 20560, USA
7. Department of Geological Sciences, University of Colorado, Boulder, CO 80309, USA
8. Department of Earth and Planetary Sciences, Northwestern University, Evanston, IL 60208, USA
9. Department of Anthropology, University of Florida, Gainesville, FL 32611–7305, USA

Corresponding author — R. Secord, email: rsecord2@unl.edu

Abstract

Body size plays a critical role in mammalian ecology and physiology. Previous research has shown that many mammals became smaller during the Paleocene-Eocene Thermal Maximum (PETM), but the timing and magnitude of that change relative to climate change have been unclear. A high-resolution record of continental climate and equid body size change shows a directional size decrease of ~30% over the first ~130,000 years of the PETM, followed by a ~76% increase in the recovery phase of the PETM. These size changes are negatively correlated with temperature inferred from oxygen isotopes in mammal teeth and were probably driven by shifts in temperature and possibly high atmospheric CO_2 concentrations. These findings could be important for understanding mammalian evolutionary responses to future global warming.

Interest in how organisms respond to climate change has intensified in recent years with projected warming of ~2° to 4°C over the next century (*1*). Although models can be developed to predict evolutionary responses to warming of this magnitude, empirical examples must be drawn from fossil or historical records. Here we report a dramatic example of shifts in body size in the earliest known horses (family Equidae) during the Paleocene-Eocene Thermal Maximum (PETM) (~56 million years ago). The PETM is recognized in marine and continental records by an abrupt negative carbon isotope excursion (CIE) that lasted ~175 thousand years (ky), caused by the release of thousands of gigatons of carbon to the ocean-atmosphere system (*2*, *3*). Some marine records suggest that although $\delta^{13}C$ values shifted rapidly at the onset of the CIE in 21 ky or less (*2*), temperature increase was slower, peaking 60 ky or more into the CIE (*4*) at ~5° to 10°C above pre-CIE levels (*5*, *6*). We use oxygen isotope values in mammal teeth as a proxy for local temperature change in the continental interior of North America, and we show that equid body size during the PETM was negatively correlated with temperature.

In extant mammals and birds (endotherms), closely related species or populations within a species are generally smaller-bodied at lower latitudes, where ambient temperature is greater (*7*). This relationship, known as Bergmann's rule, is followed by ~65 to 75% of studied extant mammals (*8*, *9*). The cause of Bergmann's rule is usually attributed to thermoregulation and the optimization of body size (*10*) and/or the availability of food resources related to primary productivity (*11*). Bergmann's rule predicts that average mammalian body size should decrease with warming climate, and smaller size in endotherms has even been suggested as a third "universal" response to warming, along with changes in phenology and species distribution (*10*). Declining body size has been attributed to warming over decadal and millennial scales in some living endotherms (*12*, *13*), but many counterexamples also exist (*10*). Furthermore, it is difficult to distinguish natural selection (genetic change) from ecophenotypic plasticity (morphological response not genetically fixed) over such short time scales. The size change documented here was, however, sustained over thousands of generations, strongly suggesting that natural selection was the cause.

Previous studies lacked the stratigraphic resolution to recognize patterns in body size change within the PETM but demonstrated gross changes in size in several mammal lineages, based on first molar tooth area (*14*, *15*). Size changes occurred in herbivorous ungulates (Perissodactyla, Artiodactyla, Condylarthra, and Tillodontia), Primates, and faunivores and omnivores (Creodonta, Carnivoramorpha, and Palaeanodonta), affecting both immigrant and endemic taxa (Figure 1). These changes conform well to Bergmann's rule in terms of the expected direction of size change. Quantifying published results, size reduction occurred in 10 Paleocene genera that ranged into the PETM, representing 38% of the range-through genera. This was followed by post-PETM size increases in eight of these genera, indicating that body size response was strongly taxon-specific (Figure 1 and table S7). Post-PETM size increases also occurred in an additional eight genera, seven of which first appeared in the PETM (Figure 1). Together these 16 genera represent a size increase in 40% of PETM genera that ranged into post-PETM biozone Wa-1 (Figure 2).

Sifrhippus [formerly *Hyracotherium* (*16*)] first appeared in North America and Europe during the PETM. Because of the lack of a plausible ancestor on these continents, it is widely thought to be an immigrant that crossed high-latitude dispersal routes opened by PETM warming (*17*). We use *Sifrhippus* to document mammalian body size change within the PETM. *Sifrhippus* is the most abundantly represented genus in new collections from the Cabin Fork area (~10 km^2) of the southern Bighorn Basin, Wyoming, and the only one for which detailed stratigraphic and quantitative morphological data are available. We also isotopically sampled *Sifrhippus*, *Coryphodon* (Pantodonta; large archaic herbivorous ungulates), and *Ectocion* and *Copecion* (phenacodontid condylarths; herbivorous ungulates of uncertain affinities). The PETM at Cabin Fork is represented by a ~35-m-thick sequence of fluvial mudstones, floodplain soils (paleosols), and fluvial sandstones. We constructed an age model that assumes varying rates of sediment accumulation: Avulsion deposits (mudstones and thin sandstones) represent fast rates, and paleosols represent much slower rates [see the supporting material (SM)]. Local sections were correlated to a composite section (Figure 2) using marker beds traced with a differential Global Positioning System unit (SM).

The CIE at Cabin Fork is recorded in the carbonate component of mammalian tooth enamel ($\delta^{13}C_E$) (Figure 2, A and B) and in bulk organics and leaf wax *n*-alkanes (*6*, *18*). $\delta^{13}C_E$ in mammalian herbivores reflects the $\delta^{13}C$ value of the vegetation they consume, with predictable enrichment (*19*). Plants in turn track the $\delta^{13}C$ value of atmospheric CO_2, with influences from environmental factors such as humidity and vegetation density (*20*, *21*). At Cabin Fork, phenacodontids (*Ectocion* and *Copecion*) record a negative shift of ~4.6 per mil (‰) in $\delta^{13}C_E$ at the onset of the CIE (Figure 2A). This is consistent with estimates of atmospheric change of ~4.6‰ during the PETM from a leaf discrimination model (*20*) and ~4.0‰ from modeling of marine carbonate dissolution (*2*), indicating that phenacodontid $\delta^{13}C_E$ is primarily tracking atmospheric $\delta^{13}C$ values, rather than environmental change.

Sifrhippus sandrae first appears at Cabin Fork near the base of the lowest intermittent red bed (LIRB) at 14.5 m (Figure 2). The onset of the CIE in most mammal teeth also begins at the base of the LIRB (Figure 2, A and B) but is recorded slightly lower (13.75 m) in dispersed bulk organics. The oldest specimens of *S. sandrae* had an average body size of ~5.6 kg, based on first lower molar area. Body size in *S. sandrae* progressively decreased from its first appearance at 14.5 m to the 41-m level, with a total reduction of ~30% over ~130 ky ($P < 0.001$) (Figure 2D and SM). Individuals at 41 m had an average body weight of ~3.9 kg and are among the smallest known horses. The dwarfing of *S. sandrae* was followed by a ~76% increase in body size during the recovery phase of the CIE, to an average size of ~7.0 kg (Figure 2D).

The mode of evolution (random, static, or directional) for *Sifrhippus* body size change was determined using a moving window log rate interval (mwLRI) analysis, which is a modification of the standard LRI analysis (*22*) (SM). Both methods assume that rates of change in a time series variable are inversely proportional to the interval of time over which rates are measured, because of the occurrence of small reversals in the variable. The relationship between rates of change and the lengths of intervals over which they are observed is used to determine evolutionary mode (*22*). Our mwLRI results indicate with 95% confidence that *Sifrhippus* body size directionally decreased from its first appearance to the 41-m level, after which stratigraphic resolution and sample sizes are insufficient to distinguish between directional and random evolutionary change. Thus, *Sifrhippus* experienced sustained selection for diminutive body size for ~130 ky.

To test whether body size change in *Sifrhippus* is significantly correlated with temperature, as predicted by Bergmann's rule, we used $\delta^{18}O$ values in *Coryphodon* enamel ($\delta^{18}O_E$) as a proxy for change in mean annual temperature (MAT). *Coryphodon* was a large water-dependent or semi-aquatic mammal (*21*, *23*). Studies of ecologically similar living mammals have shown that their $\delta^{18}O_E$ faithfully records the $\delta^{18}O$ of surface water (*24*, *25*), which in turn is strongly correlated with air temperature at mid- to high latitudes (*26*). *Sifrhippus* first lower molar area is negatively correlated with *Coryphodon* $\delta^{18}O_E$ values ($P \leq 0.05$, SM), suggesting that *Sifrhippus* body size decreased as ambient air temperature increased.

Greater aridity in the PETM could also have contributed to diminished body size by lowering primary productivity. Both floras and paleosols in the Bighorn Basin suggest increased aridity during at least parts of the PETM (*6*, *20*, *27*). To test this, we used two aridity proxies. The first is based on the difference between mean $\delta^{18}O_E$ values in aridity-sensitive and aridity-insensitive mammals (*24*). *Coryphodon* should be aridity-insensitive because of

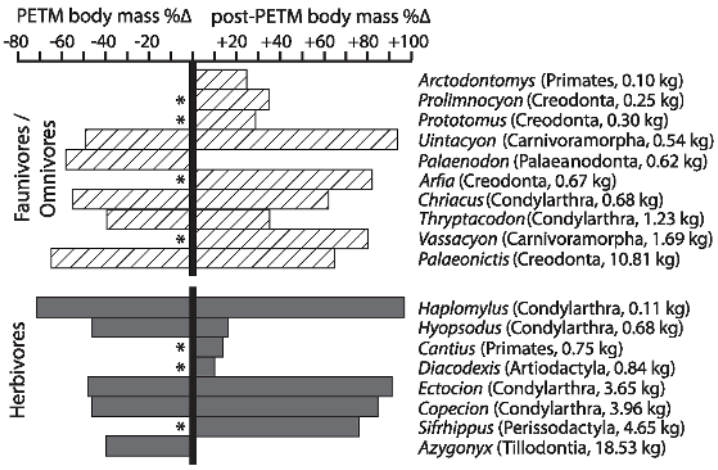

Figure 1. Summary of percent mean body size change in genera that exhibit change from the latest Paleocene to the PETM (left), and from the PETM to the post-PETM (right). No genus exhibits a size increase in the PETM or a decrease after the PETM. Compiled from published sources, except for *Sifrhippus* from this study. Asterisks indicate genera that first appear in the PETM. See table S7 for a summary of all PETM taxa and sources.

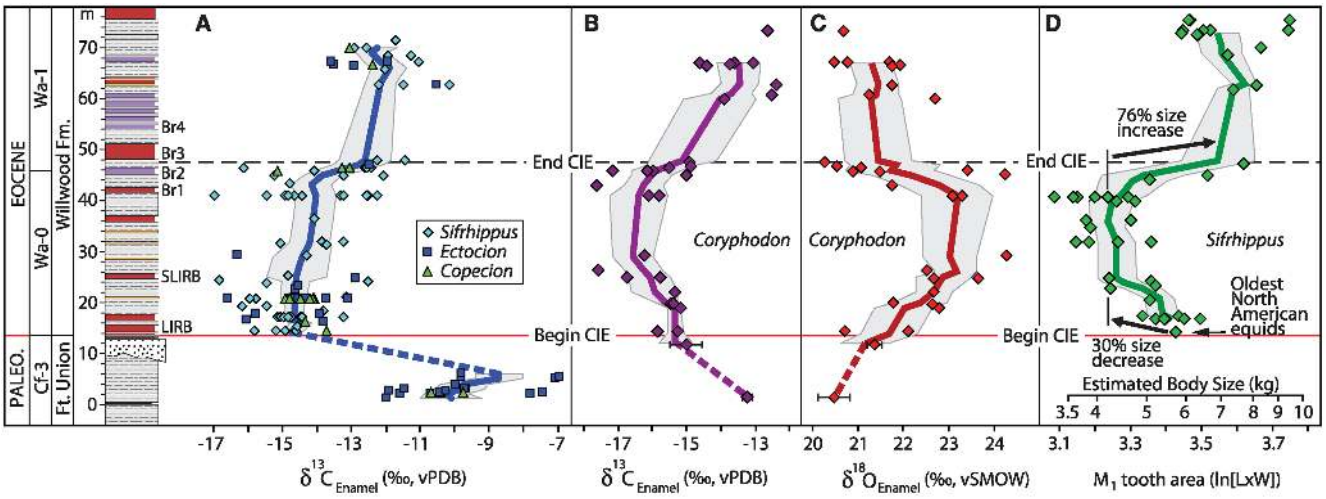

Figure 2. Comparison of PETM Cabin Fork records. (**A**) From left to right, epochs, mammalian biozones, formations, meter levels, marker beds, and $\delta^{13}C_E$ values for three common mammal genera. vPDB, Vienna Pee Dee belemnite standard. (**B** and **C**) $\delta^{13}C_E$ and $\delta^{18}O_E$ values for *Coryphodon*. vSMOW, Vienna standard mean ocean water standard. (**D**) Log-transformed measurements of first lower molar area (length × width) for *Sifrhippus*. Data points represent single individuals except where error bars (indicating 95% confidence of the mean for multiple samples from one individual) are shown. Solid colored lines show five-point moving averages; the gray area is the 95% envelope of uncertainty for each line. PALEO, Paleocene; Cf, Clarkforkian; Wa, Wasatchian. LIRB, SLIRB, and Br denote key marker beds.

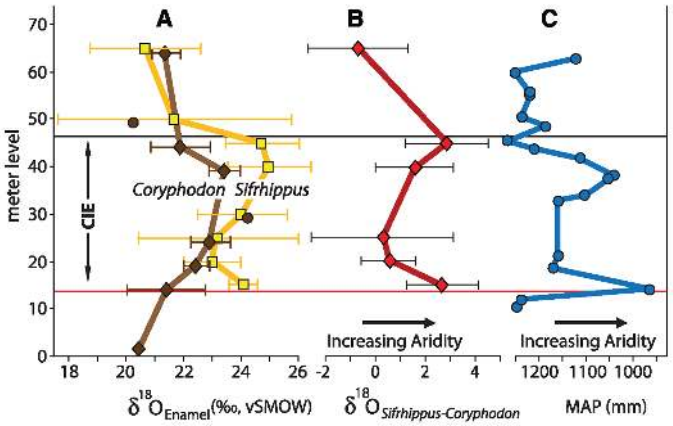

Figure 3. Aridity and precipitation proxies. (**A**) Comparison of mean $\delta^{18}O_E$ values for aridity-insensitive *Coryphodon* (brown diamonds) and aridity-sensitive *Sifrhippus* (gold squares). Data are in 5-m bins. Brown circles are singletons of *Coryphodon*. (**B**) Aridity proxy curve based on (A), showing mean differences between *Sifrhippus* and *Coryphodon* $\delta^{18}O_E$. Greater difference implies greater aridity. Error bars show 95% confidence of the mean, offset in (A) by 1 m to avoid overlap. (**C**) MAP proxy based on paleosol major oxides from a nearby correlative section (HW16 section, SM).

its probable water dependence (*21*, *23*), whereas *Sifrhippus* is the taxon most likely to be aridity-sensitive, because it has the highest average mammalian $\delta^{18}O_E$ value, suggesting that it consumed leaves in open areas where leaf water was evaporatively ^{18}O-enriched. Increased aridity should result in higher *Sifrhippus* $\delta^{18}O_E$ values and greater separation between it and *Coryphodon* $\delta^{18}O_E$ (Figure 3A). Our second aridity proxy estimates mean annual precipitation (MAP) based on paleosol major oxides (Figure 3C and SM). Both proxies suggest drier conditions at the beginning of the CIE, followed by wetter conditions starting at ~20 m (~68 ky into the PETM), with a return to drier conditions by ~38 m (~108 ky into the PETM). Overall, there is poor agreement between *Sifrhippus* body size change and the aridity proxies. Both proxies indicate a shift to wetter conditions while body size in *Sifrhippus* is decreasing, which is counter to expectations if the primary cause of dwarfing was lowered productivity caused by increased aridity.

Our results are consistent with mammalian dwarfing driven by warming, but temperature alone may be an insufficient explanation. Although body mass in living mammals is highly correlated with MAT in the Nearctic [coefficient of determination (R^2) = –0.75], this relationship weakens above ~11°C and reverses at higher temperatures in the Neotropics (*9*). MAT was well above ~11°C in the latest Paleocene and PETM of the Bighorn Basin (*6*). Furthermore, ~25 to 35% of living mammals deviate from Bergmann's rule (*8*, *9*), and it is likely that at least some mammal lineages would have gotten larger during the PETM if MAT were the only controlling factor.

Another possible cause for body size decrease in the PETM is elevated atmospheric partial pressure of CO_2 (Pco_2) (*28*), which might covary with temperature. In many extant plants, elevated CO_2 increases biomass but reduces nitrogen and protein content in leaves and can elevate phenol levels, yielding cellulose-rich vegetation that is less nutritious and harder for herbivores to digest (*29*). Ultimately, this should result in slower growth and reproductive rates in herbivorous mammals (*30*), conceivably resulting in selection for smaller body size. Although this mechanism could have reduced body size in herbivores, size also decreased among PETM carnivores (Figure 1), which must be explained by an indirect response, such as selection for smaller predators because of smaller prey (*31*). Recent modeling of rates of carbon release during the PETM shows the largest increase in Pco_2 at the onset of the CIE, followed by lower concentrations later in the event (*2*). This is inconsistent with a Pco_2-driven decrease in body size, because *Sifrhippus* was smallest near the end of the main phase of the PETM. Although elevated Pco_2 could have been a contributing factor, our results favor temperature as the primary driver of dwarfing in *Sifrhippus*.

PETM warming was similar in magnitude to that predicted by some global models over the next century (*1*) but occurred at a much slower rate and began from a warmer late Paleocene baseline. Nevertheless, some generalizations applicable to future warming may still be relevant. Diminished body size in some mammal species, along with changes in ecology and physiology, might be expected in response to warming. The pattern of dwarfing seen in the PETM mirrors recent reductions in body size in endotherms that have been attributed to anthropogenic warming (*10*, *12*). Although the rate of present warming is

much faster than during the PETM, and mammals may not respond in exactly the same manner, the dramatic response to warming observed in PETM equids provides a measure of possible responses to future warming in modern mammals.

References and Notes

1. Intergovernmental Panel on Climate Change (IPCC), *Climate Change 2007 Synthesis Report* (IPCC, Geneva, 2007).
2. Y. Cui et al., *Nat. Geosci.* 4, 481 (2011).
3. F. A. McInerney, S. L. Wing, *Annu. Rev. Earth Planet. Sci.* 39, 489 (2011).
4. G. J. Bowen, D. J. Beerling, P. L. Koch, J. C. Zachos, T. Quattlebaum, *Nature* 432, 495 (2004).
5. R. Secord, P. D. Gingerich, K. C. Lohmann, K. G. Macleod, *Nature* 467, 955 (2010).
6. S. L. Wing et al., *Science* 310, 993 (2005).
7. E. Mayr, *Animal Species and Evolution* (Harvard Univ. Press, Cambridge, MA, 1963).
8. K. G. Ashton, M. C. Tracy, A. de Queiroz, *Am. Nat.* 156, 390 (2000).
9. M. Á. Rodríguez, M. Á. Olalla-Tárraga, B. A. Hawkins, *Glob. Ecol. Biogeogr.* 17, 274 (2008).
10. J. L. Gardner, A. Peters, M. R. Kearney, L. Joseph, R. Heinsohn, *Trends Ecol. Evol.* 26, 285 (2011).
11. B. K. McNab, *Oecologia* 164, 13 (2010).
12. V. Millien et al., *Ecol. Lett.* 9, 853 (2006).
13. F. A. Smith et al., *Global Planet. Change* 65, 122 (2009).
14. P. D. Gingerich, *Univ. Mich. Pap. Paleontol.* 28, 1 (1989).
15. W. C. Clyde, P. D. Gingerich, *Geology* 26, 1011 (1998).
16. Numerous authors have shown the use of "*Hyracotherium*" to be invalid for North American equids. Thus, the species *"Hyracotherium" sandrae* (PETM) and *"H." grangeri* (post-PETM) were assigned to the new genera *Sifrhippus* Froelich 2002 and *Arenahippus* Froelich 2002, respectively. We found, however, that characters used to separate *Sifrhippus* from *Arenahippus* are highly variable and not useful for generic identification. Thus, we refer both species to *Sifrhippus* pending formal revision.
17. P. L. Koch, J. C. Zachos, P. D. Gingerich, *Nature* 358, 319 (1992).
18. F. A. Smith, S. L. Wing, K. H. Freeman, *Earth Planet. Sci. Lett.* 262, 50 (2007).
19. B. H. Passey et al., *J. Archaeol. Sci.* 32, 1459 (2005).
20. A. F. Diefendorf, K. E. Mueller, S. L. Wing, P. L. Koch, K. H. Freeman, *Proc. Natl. Acad. Sci. U.S.A.* 107, 5738 (2010).
21. R. Secord, S. L. Wing, A. Chew, *Paleobiology* 34, 282 (2008).
22. P. D. Gingerich, *Genetica* 112–113, 127 (2001).
23. M. T. Clementz, P. A. Holroyd, P. L. Koch, *Palaios* 23, 574 (2008).
24. N. E. Levin, T. E. Cerling, B. H. Passey, J. M. Harris, J. R. Ehleringer, *Proc. Natl. Acad. Sci. U.S.A.* 103, 11201 (2006).
25. J. D. Bryant, P. N. Froelich, *Geochim. Cosmochim. Acta* 59, 4523 (1995).
26. W. Dansgaard, *Tellus* 16, 436 (1964).
27. M. J. Kraus, S. Riggins, *Palaeogeogr. Palaeoclimatol. Palaeoecol.* 245, 444 (2007).
28. P. D. Gingerich, *Trends Ecol. Evol.* 21, 246 (2006).
29. P. Stiling, T. Cornelissen, *Glob. Change Biol.* 13, 1823 (2007).
30. C. E. Owensby, R. C. Cochran, L. M. Auen, in *Carbon Dioxide, Populations, and Communities*, C. Koerner, F. Bazzaz, Eds. (Academic Press, San Diego, CA, 1996), pp. 363–371.
31. S. G. B. Chester, J. I. Bloch, R. Secord, D. M. Boyer, *J. Mamm. Evol.* 17, 227 (2010).

Acknowledgments — We thank T. Bown, P. Gingerich, B. MacFadden, K. Rose, E. Sargis, and S. Strait for helpful discussions and advice; J. Curtis, B. Tucker, and A. Baczynski for help with isotope lab work; J. Bourque and A. Hastings for specimen preparation; and P. Koch and two anonymous reviewers for helpful comments.

Supported by NSF grants EAR-0640076 (J.I.B., J.K., R.S.), EAR-0719941 (J.I.B.), EAR-0717892 (S.L.W.), EAR-0718740 (M.J.K.), and EAR-0720268 (F.A.M.).

Supporting Materials follow.

Materials and Methods

Composite Lithostratigraphic Section Construction

A composite lithostratigraphic section was constructed for fossil localities over a geographic area of ~10 km^2 collectively called Cabin Fork, for the Cabin Fork drainage of the southern Bighorn Basin, Wyoming. This composite section allowed fossil and geochemical data to be placed into a chronologic sequence. Local sections were correlated using several geographically extensive marker beds (Fig. 2A). Initially, most of these beds were identified in what we termed the "master section" in the "Prong Point" area of Cabin Fork (Fig. S1). Many of the diagnostic lithologic features of these marker beds were recognized at Prong Point, including, but not limited to, color, grain size, presence of paleosol nodules and/or ferruginous nodules, bed thickness, and thickness of intervals separating beds. Marker beds were physically traced from the master section and their 3-dimensional positions were recorded using a differential GPS. This allowed observation of which lithologic features were variable and which ones were more constant. With an understanding of the diagnostic features of single beds and sequences of beds in the master section, we were often able to identify particular marker beds prior to physically tracing them to the master section. In almost all regions of our collecting area are now connected by overlapping bed traces. Our collecting was later expanded to include higher and lower stratigraphic levels. Our "Highway 16" section (Fig. S1) includes the upper levels of the original master section as well as extensive stratigraphy above it.

Bed traces and localities were recorded using a high resolution differentially corrected GPS unit. Specifically we used a Trimble ProXRS in the early years of the

project, and later switched to a Trimble GeoXT. Both units are rated for sub-meter accuracy in geographic coordinates using the WAAS signal and through real-time or post-processing corrections of satellite errors as compared to known base stations. Elevation reading accuracy is reportedly less than 2.5 meters. By repeatedly recording the same position from one year to the next over this seven year project we found that accuracy was usually at least as good as reported and in many cases it was even better in both geographic and elevational readings. Furthermore, elevational readings taken in the same recording session were often more accurate based on comparison with Jake-staff measured sections. GPS readings and Jake-staff measurements were highly correlated (r^2 = 0.99) and were almost always in good agreement (Fig. S2) for stratigraphic position of individual beds and for total section thicknesses (often less than 25 cm difference). Thus, this system was exemplary for digitally recording the stratigraphic position of fossil localities relative to marker beds.

We treated stratigraphy of local sections as being flat-lying although on average a dip of 1-3 degrees was present. Error introduced was negligible compared to error in elevational GPS measurements.

Extensive bed tracing indicated dramatic changes in marker bed thickness as well as in the stratigraphic thickness separating marker beds. This means that absolute stratigraphic position of fossil localities relative to a single marker bed were often not meaningful in terms of the chronology of fossil localities from other parts of the field area (unless the fossil occurred at the very bottom of a marker bed). Therefore we converted stratigraphic distances to proportions (e.g., a locality's position is reported as above the top of Br2 by 20% the distance between Br2 and Br3). The limitation with this

method is that localities can only be unambiguously placed if they are within a marker bed or if they are bracketed by at least two marker beds. However, in most cases data on bracketing beds was obtainable. Finally, relative stratigraphic positions of all localities were transformed into absolute meter levels shown in the composite section using marker bed levels in the master section as a base (Fig. 2A).

Mean Annual Precipitation Estimates from Paleosols

The paleosols in a section near Wyoming Highway 16 (HW16 section), about 13 km northwest of the main Cabin Fork area, were used as a proxy for mean annual precipitation (MAP). The HW16 section was correlated to the CAB10 composite section (Fig. 2) using $\delta^{13}C$ values in organic matter and marker beds. Location information for the paleosols is given in Table S1.

Quantitative estimates of MAP were calculated using the CALMAG weathering index of Nordt and Driese (*1*). This method, developed especially for Vertisols, is appropriate because the Willwood paleosols are paleo-Vertisols. If paleosols were thicker than 1 m, the upper part of the B horizon was sampled at 10 cm vertical intervals for geochemical analysis (*2*). Fewer samples were collected from B horizons of thinner paleosols (<1 m thick). Samples were analyzed for major element oxides using a Kevex 0700 x-ray fluorescence spectrometer at the University of Colorado Laboratory for Environmental and Geological Studies (LEGS). Weight percents given by x-ray fluorescence (XRF) were recalculated to molar percents for use in chemical weathering analyses. CALMAG was calculated for each of these samples, and MAP was calculated from the CALMAG values, following the approach of Nordt and Driese (*1*). For

paleosols with multiple samples, the mean MAP value was calculated. Results are shown in Fig. 3C and Table S1.

Age Model

The Willwood Formation consists of two facies: paleosols and heterolithic avulsion deposits. Moderately to strongly developed paleosols formed on mudrocks deposited by overbank flooding. The paleosols alternate vertically with the heterolithic deposits consisting of mudrocks, which show minimal paleosol development, and thin sandstones. The heterolithic deposits are interpreted to be ancient avulsion belt deposits that formed on the floodplain as the main channels were episodically abandoned in favor of new channel courses (*3*).

Limited pedogenic development indicates that the avulsion deposits accumulated very quickly compared to the paleosols, and this is supported by study of modern avulsion deposits (*4*). Consequently, we assigned 10^3 years for each meter of avulsion deposit. The total time represented by avulsion deposits (25 x 10^3 years) was subtracted from total time estimated for the CIE (175 x 10^3 yr), yielding 150 x 10^3 yr for the total time represented by the eleven paleosols in the CIE interval (Table S2).

Various studies have used chronosequences to assess the profile development of Quaternary soils to soil age (*5*). These studies quantify particular morphologic features to generate an index that reflects the degree of soil development. Some features the indices use are not readily available to paleosol studies (e.g., moist and dry consistence). Other properties, such as color, are influenced by other soil-forming factors including climate and vegetation. More importantly, chronosequence studies analyze soils that develop in a

top down manner, because the surface is stable and soil depth and the degree of alteration increase over time. In contrast, alluvial paleosols undergo what Johnson and Watson-Stegner (*6*) termed regressive processes that impede soil development. Such processes include surface erosion and incorporation of new parent material at the top of the soil because of episodic floodplain deposition.

Because of the difficulties in developing a robust index of development for the Willwood paleosols, we used thickness of the B horizon as an estimate of the time represented by a particular paleosol. Focusing on the B horizon eliminates problems with erosion of all or part of the A horizon. The thickness of the B horizon reflects both downward migration of the lower soil boundary due to weathering of alluvium and upbuilding of the soil through time as a result of continued floodplain aggradation that was accompanied by pedogenesis. The thickness of the B horizon represents the length of time that sediment accumulation was slow and steady. For example, a 2 m thick B horizon indicates that the floodplain aggraded slowly over a relatively long time. Eventually, channel avulsion deposited several meters of sediment on top of the soil and that halted its development (*3*). In contrast, a 0.5 m thick B horizon represents slow floodplain accumulation for a commensurately shorter period of time before an avulsion event stopped its development.

Dividing 150 x 10^3 yr by total thickness of the B horizons of the 11 paleosols in the interval (8.65 m), means that each meter of soil B horizon represents ~17,341 yr (Table S2). A time stratigraphic column was constructed using the stratigraphic position of each paleosol and avulsion deposit in the section and the time assigned to each paleosol and avulsion deposit (Table S3). The base of LIRB, which marks the base of the

CIE, is at 14.45 m in the section and at 0 years. The top of the CIE section is at the base of BR3 at the 48.05 m level in the section. It corresponds to a 175 x 10^3 yr duration for the CIE in the time stratigraphic section.

Moving Window Log-Rate-Interval Analysis (mwLRI)

Optimal binning search.—An exhaustive search was performed to find the binning scheme that optimized two criteria: (1) the maximum the number of time intervals with N > 1, and (2) the minimum number of intervals with N =1. The search was conducted using an algorithm written in the R statistical computing package (*7*) that allowed the bin duration to vary from 0.2 kyr to 50 kyr at increments of 0.2 kyr. The beginning, or start value, of each binned series was also incrementally shifted forward by 0.2 ky with the constraint that the first M/1 value of the morphological time series was always contained within the first bin, resulting in multiple binning schemes at each value of bin duration. For each set of binning schemes at a particular bin duration, the algorithm would report either the single scheme that optimized the above criteria, or, in the case of multiple, equivalently-optimized schemes, the binning scheme with the median start value. Out of the reported binning schemes, an 18.6 ky binning scheme was chosen, providing 12 bins with N > 1 and 3 bins with N = 1 for a total of 15 time steps. The moving window LRI analysis was applied to this binned version of the M/1 crown area time series.

Description of moving window log-rate-interval method.—The moving window log-rate-interval (mwLRI) analysis is an extension of the standard LRI analysis of Gingerich (*8*) in which the relationship between rates of change and the lengths of

intervals over which they are observed is used to investigate time series dynamics (i.e., patterns of directional trends and stable values) . The LRI method is built on the observation that rates of change in a time series variable are often inversely proportional to the interval of time over which each rate is measured (*8-11*) which is primarily due to the occurrence of reversals in a given time series. It should be noted here that this relationship holds true regardless of whether the interval length is measured in time or depth. Thus, the phrase "time series" is used here to refer to variables measured over either numerical time or stratigraphic depth.

In an LRI analysis, all possible pairwise rates of change are regressed onto the corresponding interval of time and a slope is calculated for the regression line. The steepness of the negative slope reflects the amount of reversals present in a time series, such that a directional time series with few reversals would produce a ~ 0 slope value and a stable time series with many reversals would produce a slope value near -1. The expected slope value for an unbiased, random walk is -0.5, but actual slope values derived from random walks can vary anywhere between 0 to -1.

The mwLRI analysis includes two additions to the standard LRI method. First, the observed slopes in each mwLRI analysis are compared to distributions of slopes generated using Monte Carlo simulations of a random walk. This is done in order to reject a null hypothesis of a random time series and unequivocally determine if the observed time series exhibits directional change or stability. Each Monte Carlo simulation starts with the initial time step of the observed time series and randomly adds or subtracts a value from a uniform distribution that ranges from minimum to the maximum observed differences between consecutive steps in the observed series.

Choosing from such a uniform distribution constrains the amount of change possible between consecutive steps in the random walk to be similar to that of the observed time series. The number of time steps in the resulting random walk is equal to that of the observed time series. If the observed slope falls outside and above confidence intervals of slopes produced by random walks, the observed time series can be interpreted as exhibiting directional change. An observed slope outside and below a given confidence interval is indicative of a stable time series.

The second addition to the standard LRI method is that a mwLRI analysis performs a heuristic search for shift points in time series dynamics (i.e., changes in directionality or mode). A standard LRI analysis of a time series with heterogeneous dynamics requires *a priori* hypotheses concerning when changes in directionality or mode take place. The heuristic search approach of the mwLRI method avoids this prerequisite by calculating an LRI slope for all possible subsets of the observed time series, allowing each slope and its statistical significance to be interpreted within the context of all other subset results. Operationally, this is performed by calculating an observed LRI slope and a distribution of random walk slopes in a window that varies from a minimum of 5 steps to the length of the entire series. After each calculation, the test window shifts one step forward in the time series and performs a new set of calculations. Once all possible consecutive subsets are tested at a given window size, the window size increases by one step, and the process is reiterated. A minimum window size of 5 time steps was chosen to provide at least 10 points for the slope calculation.

Result "maps" in which LRI results for subsets are organized by initial time step and window size (Fig. S3) provide a useful way of applying mwLRI results to a final

interpretation of dynamics in the observed time series. A long subset of homogeneous dynamics (e.g., a long directional trend) in a time series analyzed in windows smaller than or equal to the length of the homogenous subset is likely to produce nested and similar slope and significance values, appearing as a cluster of similar results on the map. For consistency, only the value with the greatest window size is reported in the final interpretation. Temporally adjacent subsets exhibiting different time series dynamics are likely either to overlap or be separated by a series of time steps that cannot be distinguished from a random walk. In these cases, the midpoint of the overlap or random subset is interpreted as the shift point in the observed time series dynamics.

The version of the mwLRI analysis used here was performed using an R script that is available upon request. Results for our analysis of *Sifrhippus* are shown in Fig. S4.

Regression Analyses

We used ordinary least squares linear regression to determine if relationships existed among *Sifrhippus* first lower molar (M/1) size, *Coryphodon* $\delta^{18}O$ values, and *Sifrhippus* $\delta^{18}O$ values. The Durbin-Watson statistic was used to test for serial correlation (autocorrelation) in the datasets, which is sometimes present in time series (*12-16*). When serial correlation is present, the regression errors (residuals) are correlated with themselves lagged by one or more units. Serial correlation violates the assumption of independence. Positive serial correlation results in an underestimate of the error variance resulting in a lower probability (*P*-value) estimate and an overly optimistic conclusion, while negative serial correlation tends to overestimate the error variance. We used the Durbin-Watson statistic (DW) to test for first order serial correlation in the regression residuals. The Durbin-Watson test uses the difference between successive regression

residuals to approximate the amount of serial correlation present (*17, 18*). DW values range from 0 to 4. A value of 2 indicates the absence of serial correlation, while values of 0 and 4 indicate strong positive and negative serial correlation, respectively. Upper and lower critical values have been calculated for the Durbin-Watson statistic based on sample size and the number of independent variables in the regression (*13*). If DW is greater than the upper critical value, the null hypothesis of serial correlation can be rejected with 95% confidence. If it is below the lower critical value, serial correlation is probably present. If it falls between critical values, the presence of serial correlation is uncertain. We also used the Shapiro-Wilk test for normality of distribution, assuming that samples with $P \geq 0.05$ were normally distributed.

Data were placed in stratigraphic bins to test for correlation. In order to determine whether correlation was sensitive to binning schemes we conducted correlation tests using 4, 5, and 6 meter bin sizes, and shifted the starting points for each bin by a meter. Results are summarized in Tables S6, S7, and S8. *Sifrhippus* M/1 area is strongly correlated with *Coryphodon* $\delta^{18}O_E$ values (Table S4). Correlation is significant with 95% confidence for all in all cases, indicating that the correlation is not sensitive to binning. For all 5-meter bins and all but one 6-meter bin the DW statistic indicates that the influence of first order autocorrelation can be rejected. For two or four 4-meter bins and one 6-meter bin the DW statistic falls into the uncertain range. This is of little concern, however, given the indicated absence of autocorrelation for the large majority of bins. The Shapiro Wilk statistic indicates that the distribution of data does not differ significantly from normal for all bins. Thus, we conclude that this is a robust correlation

and there is a strong relationship between *Sifrhippus* M/1 area and *Coryphodon* $\delta^{18}O_E$ values (Table S4).

Regression of *Sifrhippus* M/1 area on *Sifrhippus* $\delta^{18}O_E$ values yielded mixed results (Table S5). The significance of the correlation is dependent to some extent on the starting point of the bin. Also problematic, the in seven of fifteen cases the DW statistic falls in the range of uncertainty, indicating that the influence of autocorrelation cannot be confidently rejected, although in no case does the statistic fall below the critical lower value. The problem seems to be worse with smaller bin sizes. Also, in several cases, distributions differ significantly from normal according to the Shapiro-Wilk statistic. When these cased were tested with rank-order tests, none was significant. Thus, this correlation is marginal. This is not especially surprising since oxygen isotopes in taxa that consume leaf water are expected to be more variable than in those that are insensitive to aridity. As discussed in the main text, *Sifrhippus* is the most likely of the common PETM taxa to have been aridity sensitive, and changes in its body size do not appear to be correlated with aridity.

Faunal (*Ectocion*, *Copecion*, *Sifrhippus*) $\delta^{13}C_E$ values are significantly correlated with *Coryphodon* $\delta^{18}O$ values in all but one case, which is marginally significant (P = 0.54). Thus, this relationship is not dependent on binning scheme. Also, the possibility of influence from first order autocorrelation can be reject in all cases, based on the DW statistic. The Shapiro-Wilk statistic does indicate deviation from normality in four of fifteen cases in the 4-meter and 5-meter binning schemes (Table S6). When Spearman's non-parametric rank order test is applied only one of these cases (4-meter bin, start 0) remains significant with 95% confidence (P = 0.043; others 0.099, 0.108, 0.214).

Nevertheless, in all cases but one that pass the Shapiro Wilk test the correlation is significant. Thus, there appears to be a relationship between faunal $\delta^{13}C_E$ values and *Coryphodon* $\delta^{18}O_E$ values. This may be expected if *Coryphodon* $\delta^{18}O_E$ values were tracking temperature changes caused by CO_2 forcing, which would be reflected in the shift to more negative $\delta^{13}C_E$ values as massive amounts of isotopically ^{13}C-depleted CO_2 were released to the atmosphere during the CIE. However, although few would argue that CO_2 forcing from highly C^{13}-depleted carbon released during the PETM was an important factor in warming during the PETM, alone it may not have been sufficient to explain the full magnitude of inferred warming (*19*).

Estimates of Mammalian Body Mass

Previous work has shown a strong correlation between molar size and long bone length (used only for *Palaeanodon*), and body mass in extant mammals (*20-28*). We used primarily equations provided by Legendre (*20*) to calculate percent changes in body mass for PETM taxa (Table S7). Many of these species are known from only a small number of fragmentary specimens, and individual estimates could change considerably with additional material and further taxonomic study. Locomotor behavior in Table S7 is speculative for some taxa. Notably, no postcrania are known for *Arctodontomys* and arboreality is assumed because other plesiadapiform primates for which postcrania are known are arboreal. Rose (*29*) suggested that *Arfia* was cursorial/scansorial. *Vassacyon* was assumed to be arboreal by Heinrich and Houde (*30*). *Hyopsodus* postcrania are not well known from the Wasatchian, but the postcrania of younger species suggest that it was a generalist, with some characters suggesting terrestriality and others suggesting the

ability to climb trees or dig (*31*). *Azygonyx* also exhibits a mosaic of terrestrial and arboreal postcranial characters (*29*).

Stratigraphic data for *Sifrhippus*, the most abundantly represented PETM genus in the Cabin Fork area, are shown in Table S8. Equid teeth were carefully examined to insure that no deciduous juvenile teeth were included. We used juvenile specimens with deciduous teeth to aid in identification of tooth position, and also considered the degree of wear to ensure that all teeth included in Table S8 belonged to adults.

Stable Isotope Analysis

Isotope ratios are expressed in delta notation as parts per thousand (‰) relative to a standard: $\delta^{18}O$ or $\delta^{13}C = ([R_{sample}/R_{standard}]-1)) \times 10^3$, where $R=^{18}O/^{16}O$ for oxygen, relative to vSMOW (Vienna standard mean ocean water), and $R=^{13}C/^{12}C$ for carbon, relative to vPDB (Vienna PeeDee Belemnite).

Oxygen and carbon stable isotopes ratios were measured from the carbonate component of mammalian tooth enamel (hydroxylapatite). Samples weighing 3-4 mg were drilled from teeth using a Brassler dental drill with a 1 mm diamond burr mounted under a binocular microscope in the Bone Chemistry Laboratory in the Department of Anthropology at the University of Florida. Samples were then pretreated with 2-3% sodium hypochlorite and 1 M acetic acid buffered with calcium acetate to remove organic matter and non-structural carbonate following the recommendations of Koch et al. (*32*). Our protocol differed only in that samples were roasted after pretreatment at 200 ºC under vacuum for 1 hour to remove volatile contaminants and water, rather than being lyophilized (*33*).

Stable isotope ratios were measured in the Light Stable Isotope Mass Spec Lab (LSIMSL) at the University of Florida in the Department of Geological Sciences. The first two batches of enamel (SB1 and SB2) were analyzed using a VG / Micromass PRISM Series II isotope ratio mass spectrometer with an Isocarb common acid bath preparation device. Samples were loaded into stainless steel boats and placed into a 44-position Isocarb preparation system. Samples were reacted in a common acid bath in orthophosphoric acid at 90° C and water was cryogenically removed in a methanol slush. Evolved CO_2 gas was measured online with the VG / Micromass PRISM Series II isotope ratio mass spectrometer. Analytical precision is generally better than ±0.1‰ for $\delta^{13}C$ and 0.1‰ for $\delta^{18}O$ at LSIMSL for the international standard NBS-19. Reported error in this section is one standard deviation (SD). Eight standards were run with each thirty-six research samples. Intralab enamel standards of LOX (modern African elephant enamel) and MES (mammoth fossil enamel) were also analyzed with each batch. These standards yielded the following values for the acid bath: LOX $\delta^{13}C$ = -5.8±0.04‰, $\delta^{18}O$ = 30.7±0.09‰ (n = 8); MES $\delta^{13}C$ = -9.8±0.07‰, $\delta^{18}O$ = 22.4±0.10‰ (n = 7).

The remaining batches were analyzed using a Finnigan-MAT 252 isotope ratio mass spectrometer coupled with a Kiel III carbonate preparation device. Oxygen and carbon isotopes were measured by reacting samples in orthophosphoric acid at 70° C using a Finnigan-MAT Kiel III carbonate preparation device. Evolved CO_2 gas was measured online with a Finnigan-MAT 252 mass spectrometer. Analytical precision for isotope analyses is generally better than ±0.05‰ for $\delta^{13}C$ and 0.10‰ for $\delta^{18}O$ for the NBS-19 standard at LSIMSL. Our enamel standards yielded: LOX $\delta^{13}C$ = -5.8±0.06‰, $\delta^{18}O$ = 31.2±0.09‰ (n = 12); MES $\delta^{13}C$ = -9.9±0.09‰, $\delta^{18}O$ = 22.6±0.17‰ (n = 29).

Differences between samples run on the PRISM Series II (acid bath) and Finnigan-MAT 252 (Kiel) ranged from 0.05 to 0.13‰ (LOX and MES, respectively) for enamel $\delta^{13}C$, and 0.52 to 0.20‰ (LOX and MES, respectively) for enamel $\delta^{18}O$. While the difference in $\delta^{13}C$ for MES was significant ($P<0.001$) it is trivial at the scale at which we are working and no correction was made. The differences in $\delta^{18}O$ were greater, especially for LOX, and both were significant ($P<0.001$). These differences appear to scale with a greater difference at the higher $\delta^{18}O$ values for LOX. Assuming the relationship is linear, a correction factor would be $\delta^{18}O_{Kiel} = \delta^{18}O_{Acid\text{-}Bath} \times 1.038 - 0.6507$. Because our $\delta^{18}O$ values for Bighorn Basin enamel are most similar to those of the MES standard, this correction results in only a small difference (average = -0.20‰). This difference is minor for the scale at which we are working and only slightly more than one standard deviation for the MES standard for the Kiel (±0.17‰; n = 29). Therefore we refrained from making a correction. Values for our Bighorn Basin fossil material are reported in Table S9.

References

1. L. C. Nordt, S. D. Driese, *Geology* **38**, 407 (2010).
2. S. G. Driese, *Journal of Geology* **112**, 543 (2004).
3. M. J. Kraus, B. Gwinn, *Sedimentary Geology* **114**, 33 (1997).
4. N. D. Smith, T. A. Cross, J. P. Dufficy, S. R. Clough, *Sedimentology* **36**, 1 (1989).
5. J. W. Harden, *Geoderma* **28**, 1 (1982).
6. D. L. Johnson, D. Watson-Stegner, *Soil Science* **143**, 349 (1987).
7. R_Development_Core_Team, 2011, http://www.R-project.org.
8. P. D. Gingerich, *American Journal of Science* **293A**, 453 (1993).
9. W. C. Clyde, P. D. Gingerich, *Paleobiology* **20**, 506 (Fal, 1994).
10. P. D. Gingerich, *Genetica* **112-113**, 127 (2001).
11. P. D. Gingerich, *Annual Review of Ecology, Evolution, and Systematics* **40**, 657 (2009).
12. R. H. Shumway, *Applied statistical time series analysis*. (Prentice Hall, New Jersey, 1988), pp. 379.
13. R. H. Shumway, D. S. Stoffer, *Time series analysis and its applications*. (Springer-Verlag, New York, 2000), pp. 549.
14. M. L. McKinney, in *Evolutionary trends,* K. J. McNamara, Ed. (The University of Arizona Press, Tucson, 1990), pp. 28-58.
15. J. J. F. Commandeur, S. J. Koopman, *An introduction to state space time series analysis*. J. Doornik, B. Hall, Eds., (Oxford University Press, Oxford, 2007), pp. 174.

16. R. Secord, *Papers on Paleontology* **35**, 1 (2008).

17. T. H. Wonnacott, R. J. Wonnacott, *Introductory statistics for business and economics*. (John Wiley and Sons, New York, ed. Second edition, 1977), pp. 753.

18. E. B. Andersen, N.-E. Jensen, N. Kousgaard, *Statistics for economics, business administration, and the social sciences*. (Springer-Verlag, Berlin, 1987), pp. 439.

19. R. E. Zeebe, J. C. Zachos, G. R. Dickens, *Nature Geoscience* **2**, (2009).

20. S. Legendre, *Palaeovertebrata* **16**, 191 (1986).

21. S. Legendre, *Revue de Paléobiologie* **6**, 183 (1987).

22. P. D. Gingerich, *American Journal of Physical Anthropology* **47**, 395 (1977).

23. P. D. Gingerich, B. H. Smith, K. Rosenberg, *American Journal of Physical Anthropology* **52**, 231 (1980).

24. P. D. Gingerich, B. H. Smith, K. Rosenberg, *American Journal of Physical Anthropology* **58**, 81 (1982).

25. J. Damuth, B. J. MacFadden, Eds., *Body size in mammalian paleobiology: estimation and biological implications*, (Cambridge University Press, Cambridge, 1990), pp. 397.

26. M. Mendoza, C. M. Janis, P. Palmqvist, *Journal of Zoology* **270**, 90 (2006).

27. P. D. Gingerich, *Journal of Paleontology* **48**, 895 (1974).

28. B. J. MacFadden, *Paleobiology* **12**, 355 (1986).

29. K. D. Rose, in *Paleocene-Eocene stratigraphy and biotic change in the Bighorn and Clarks Fork basins, Wyoming,* P. D. Gingerich, Ed. (University of Michigan Papers on Paleontology 33, 2001), vol. 33,pp. 157-183.

30. R. E. Heinrich, P. Houde, *Journal of Vertebrate Paleontology* **26**, 422 (2006).

31. K. D. Rose, *The beginning of the age of mammals*. (The Johns Hopkins University Press, Baltimore, 2006), pp. 428.

32. P. L. Koch, N. Tuross, M. L. Fogel, *Journal of Archaeological Science* **24**, 417 (1997).

33. R. Secord, P. D. Gingerich, K. C. Lohmann, K. G. MacLeod, *Nature* **467**, 955 (2010).

34. P. D. Gingerich, *University of Michigan Papers on Paleontology* **28**, 1 (1989).

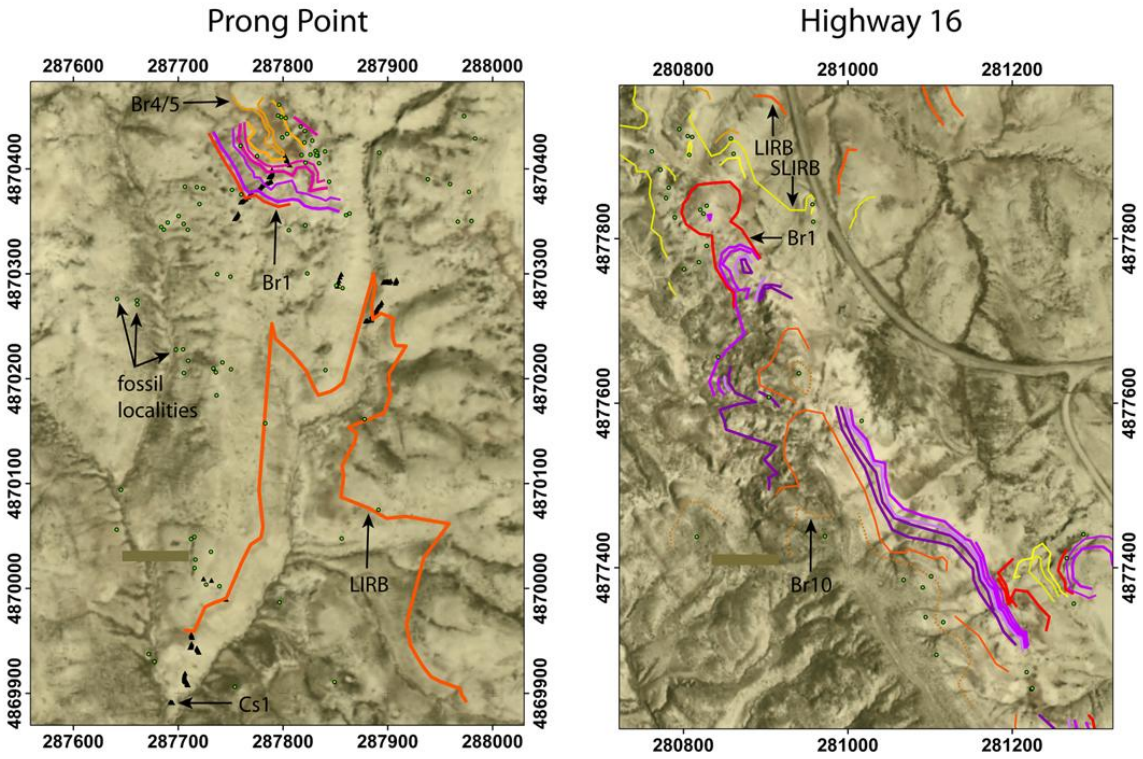

Fig. S1. Two maps showing marker bed traces in the region of our "master sections" that provide the meter levels reported in Fig. 2A. Easting and Westing coordinates are UTM's based on NAD 27 datum, Zone 13N. Colored lines indicate marker beds. Green dots represent fossil localities. Black triangles represent sample sites for geochemical analyses. Stratigraphic position was calculated using traditional Jake-staff methods as well as with differentially corrected GPS measurements. Marker beds LIRB, SLIRB, Br1, and Br4, are shown in stratigraphic sequence in Fig. 2.

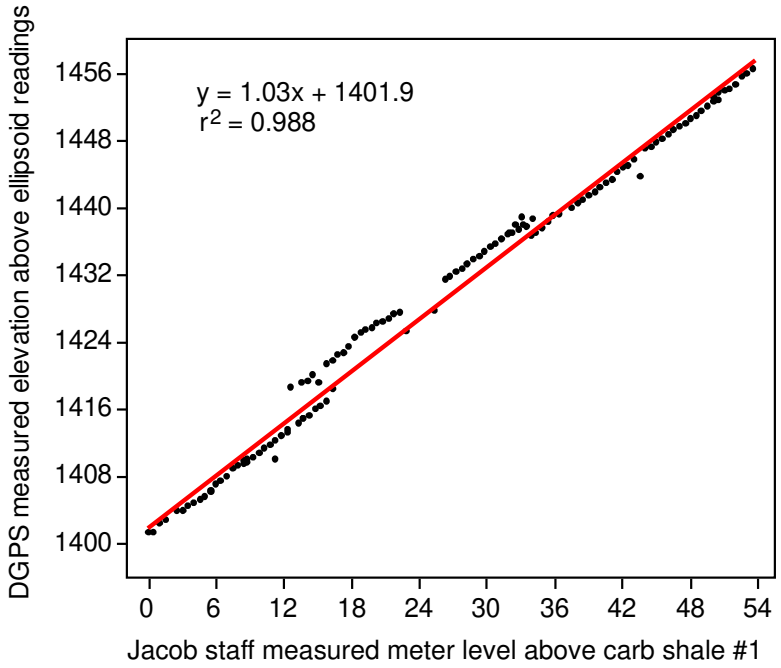

Fig. S2. Comparison of Jacob staff measurements with DGPS (Trimble ProXRS) readings. Localities whose elevations are shown here are represented by black triangles in Fig. S1, left image. Note strong correlation. Most readings were taken roughly along strike of local bedding that dips west-south-west. However, sample sites between 12 to 33 m are from local sections slightly up dip (black triangles farther to right in Fig. S1). Accordingly, the DGPS records slightly higher elevations for same bed, whereas the Jacob staff measurements have accounted for dip.

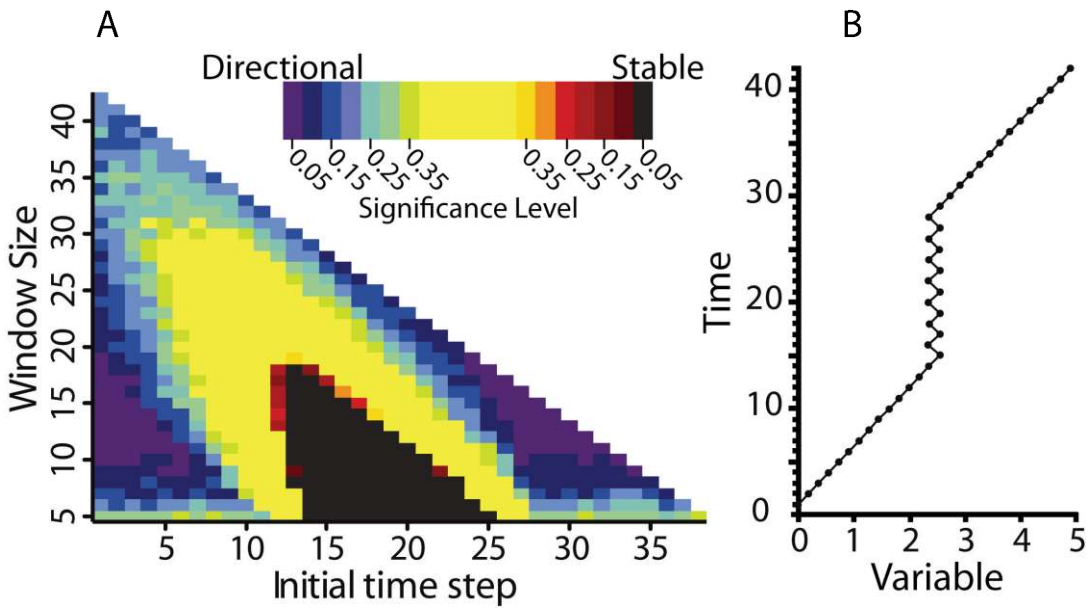

Fig. S3. Moving window LRI results for a hypothetical evolutionary time series in which two directional subsets are separated by a subset of stable values. A, colored boxes correspond to significance levels for directional, random, or stable trends. "Initial step" indicates starting point of moving window of variable size (y-axis). For example, the interval with an initial step of 3 and a window size of 12 indicates a directional trend with 95% confidence (purple). B, variable (e.g., first molar area) plotted against time. The result map (A) shows 3 clusters of 95% significant results associated with the two directional subsets (purple clusters) and the single stable subset (black cluster). Non-significant results outside of these clusters correspond to subsets of the hypothetical time series in which directional and stable patterns are mixed (e.g., time steps 10-24 or initial step 10/window size 15 in the result map). The results with the largest window size in each cluster indicate: (1) directional change from time steps 1-19, (2) stable values from time steps 13-30, and (3) directional change from time steps 24-42. Taking the midpoint of the two overlaps provides a final interpretation of the mwLRI results: directional

change between steps 1-16, stable values between steps 16-27, and directional change from steps 27-42.

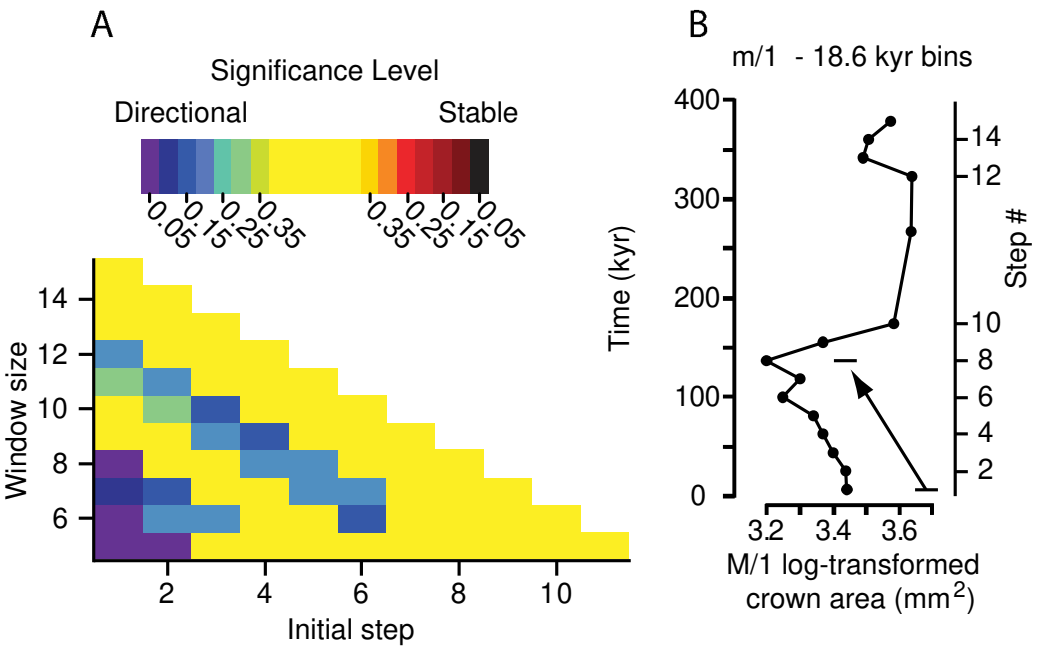

Fig. S4. Moving window LRI results of evolutionary trends in *Sifrhippus* through composite section at Cabin Fork. (A) result map of significance levels for directional, random, or stable trends. (B) Mean values of binned (-18.6 kyr bins), log-transformed, first molar area plotted against time model. Results indicate a directionally decreasing trend over steps 1-8 (~9-139 kyr interval).

Table S1. Paleosol data from Highway 16 section used to estimate mean annual precipitation. Mean values shown in boxes.

Trench	Strat Level	CALMAG	CALMAG MAP	MgO wt%	CaO wt%	Al_20_3 wt%	molar CaO	molar Al_2O3	molar MgO
HW16-08-15	64.0	65.06	1040	1.90	2.33	16.86	0.042	0.165	0.047
N44° 01.087'		72.34	1206	1.92	0.84	16.7	0.015	0.164	0.048
W107° 43.864'			1123						
HW16-08-14	61.0	75.41	1275	1.92	0.61	18.26	0.011	0.179	0.048
N44° 01.116'		74.80	1261	1.89	0.54	17.06	0.010	0.167	0.047
W107° 43.887'		75.78	1284	1.71	0.51	16.40	0.009	0.161	0.042
		72.38	1206	1.92	0.84	16.70	0.015	0.164	0.048
		73.95	1242	1.73	0.50	14.95	0.009	0.147	0.043
			1254						
HW16-08-12	56.8	72.89	1218	1.99	0.59	16.42	0.011	0.161	0.049
upper paleosol		73.21	1225	1.93	0.55	16.08	0.010	0.158	0.048
N44° 01.117'			1222						
W107° 43.881'									
HW16-08-12	56.02	72.84	1217	2.05	0.58	16.74	0.010	0.164	0.051
lower paleosol		73.33	1228	1.87	0.7	16.51	0.012	0.162	0.046
			1223						
HW16-08-08	51.53	74.51	1255	1.59	0.6	14.95	0.011	0.147	0.039
N44° 01.126'		74.49	1254	1.67	0.67	15.87	0.012	0.156	0.041
W107° 43.863'		72.72	1214	1.50	1.01	15.01	0.018	0.147	0.037
		73.35	1228	1.72	0.79	15.93	0.014	0.156	0.043
		74.31	1250	1.73	0.72	16.42	0.013	0.161	0.043
			1240						
HW16-08-07	49.6	72.93	1219	1.53	0.96	15.13	0.017	0.148	0.038
N44° 01.131'		71.10	1177	1.54	1.30	15.40	0.023	0.151	0.038
W107° 43.852'		69.97	1152	1.56	1.54	15.70	0.027	0.154	0.039
		72.54	1210	1.77	0.98	16.54	0.017	0.162	0.044
		71.40	1190	1.78	1.22	16.80	0.022	0.165	0.044
			1190						
HW16-08-06	46.45	74.78	1261	1.72	0.68	16.57	0.012	0.163	0.043

		75.28	1272	1.63	0.64	16.12	0.011	0.158	0.041
		75.17	1270	1.65	0.66	16.27	0.012	0.160	0.041
		75.10	1268	1.65	0.72	16.54	0.013	0.162	0.041
		75.70	1282	1.64	0.70	16.89	0.012	0.166	0.041
			1271						
HW16-08-05	44.8	72.28	1204	1.90	0.72	15.93	0.013	0.156	0.047
N44° 01.114'		72.97	1220	1.76	0.74	15.67	0.013	0.154	0.044
W107° 43.833'		72.72	1214	1.79	0.76	15.76	0.013	0.155	0.045
		72.79	1216	1.85	0.74	16.12	0.013	0.158	0.046
		72.73	1214	1.78	0.79	15.86	0.014	0.156	0.044
			1214						
HW16-08-02	42.74	70.85	1172	1.76	0.97	15.08	0.017	0.148	0.044
N44° 01.128'		70.01	1153	2.00	0.95	15.83	0.017	0.155	0.050
W107° 43.782'		64.22	1021	1.92	1.76	14.49	0.031	0.142	0.048
			1115						
HW16-08-01	39.14	77.90	1050	1.95	1.60	14.60	0.029	0.143	0.048
paleosol 1									
N44° 01.126'									
W107° 43.795'									
HW16-08-01	38.3	78.92	1072	1.96	1.52	14.78	0.027	0.145	0.049
paleosol 2									
HW16-08-01	34.92	69.88	1150	2.03	0.92	15.80	0.0164	0.155	0.050
paleosol 3		66.00	1062	2.20	1.28	15.32	0.0228	0.150	0.055
			1106						
HW16-08-01	33.65	69.39	1139	2.08	0.95	15.88	0.017	0.1557	0.052
paleosol 4		70.69	1168	1.97	1.00	16.43	0.018	0.1611	0.049
		70.65	1167	1.95	0.85	15.59	0.015	0.1529	0.048
		70.99	1175	1.97	0.82	15.83	0.015	0.1553	0.049
			1162						
HW16-08-17	22.03	68.41	1116	2.42	1.14	17.74	0.020	0.174	0.060
N44° 01.561'		69.91	1151	2.40	0.85	17.70	0.015	0.174	0.060
W107° 43.640'		71.95	1197	2.21	0.71	17.68	0.013	0.173	0.055
		71.05	1176	2.20	0.86	17.50	0.015	0.172	0.055
		70.88	1172	2.21	0.92	17.68	0.016	0.173	0.055

			1162						
HW16-08-19	19.39	71.68	1191	1.91	0.7	15.45	0.012	0.152	0.047
N44° 01.574'		71.29	1182	1.88	0.68	14.88	0.012	0.146	0.047
W107° 43.665'		71.25	1181	1.86	0.72	14.93	0.013	0.146	0.046
		70.20	1157	1.97	0.82	15.26	0.015	0.150	0.049
		69.87	1149	1.86	0.75	14.08	0.013	0.138	0.046
			1172						
HW16-08-19 lower	14.87	61.82	967	2.15	2.15	15.13	0.038	0.148	0.053
HW16-08-20	12.77	75.81	1284	1.68	0.57	16.58	0.010	0.163	0.042
upper paleosol		74.98	1265	1.78	0.54	16.44	0.010	0.161	0.044
N44° 01.581'		73.53	1233	1.84	0.64	16.16	0.011	0.159	0.046
W107° 43.682'		71.99	1198	1.78	0.95	16.03	0.017	0.157	0.044
		73.04	1221	1.67	0.85	15.63	0.015	0.153	0.041
			1240						
HW16-08-20	11.05	73.26	1226	1.73	0.81	16.06	0.015	0.158	0.043
lower paleosol		74.57	1256	1.75	0.66	16.54	0.012	0.162	0.044
		75.05	1267	1.74	0.62	16.65	0.011	0.163	0.043
			1250						

Table S2. Paleosol thickness and estimated time represented in CAB 10 composite section.

Paleosol	B horizon Thickness (m)	Time (years)
BR 2	1.15	19,942
BR 1	1.03	17,861
BR 0	1.28	22,196
SLIRB 4	0.42	7,283
SLIRB 3	0.36	6,243
SLIRB 2	0.23	3,988
SLIRB 1	0.36	6,243
Purple 2	0.87	15,087
Purple 1	0.23	3,988
LIRB2	1.33	23,064
LIRB1	1.39	24,104
Totals	8.65	150,000
Total soil thickness = 8.65 m		1 m = 17,341 yr
Total avulsion thick = 25.1 m		1 m = 1000 yr

Table S3. Age model based on paleosol development in CAB10 composite section.

Paleosol	Strat Base	Strat Top	thickness (m)	soil time	avulsion time	Strat Level (m)	Cumul Time (yrs)
BR6 top	54.3	54.88	0.58	10058	0	54.88	246980
Avulsion/Base BR 6	53.4	54.3	0.9	0	900	54.30	236922
BR5 top	53.19	53.4	0.21	3642	0	53.4	236022
Avulsion/Base BR 5	52.38	53.19	0.81	0	810	53.19	232380
BR4 top	51.63	52.38	0.75	13006	0	52.38	231570
Avulsion/Base BR 4	50.5	51.63	1.13	0	1130	51.63	218564
BR3 top	48.05	50.5	2.45	42485	0	50.5	217434
Avulsion/Base BR 3	44.75	48.05	3.3	0	3300	48.05	174949
BR2 top	43.6	44.75	1.15	19942	0	44.75	171649
Avulsion/Base BR 2	42.53	43.6	1.07	0	1070	43.60	151707
BR1 top	41.5	42.53	1.03	17861	0	42.53	150637
Avulsion/Base BR 1	41.14	41.5	0.36	0	360	41.50	132776
BR0 top	39.86	41.14	1.28	22196	0	41.14	132416
Avulsion/Base BR 0	24.65	39.86	15.21	0	15210	39.86	110220
SLIRB 4 top	24.23	24.65	0.42	7283	0	24.65	95010
Avulsion/Base SLIRB4	23.29	24.23	0.94	0	940	24.23	87727
SLIRB 3 top	22.93	23.29	0.36	6243	0	23.29	86787
Avulsion/Base SLIRB3	22.01	22.93	0.92	0	920	22.93	80544
SLIRB 2 top	21.78	22.01	0.23	3988	0	22.01	79624
Avulsion/Base SLIRB2	21.58	21.78	0.2	0	200	21.78	75636
SLIRB 1 top	21.22	21.58	0.36	6243	0	21.58	75436
Avulsion/Base SLIRB1	19.74	21.22	1.48	0	1480	21.22	69193
Purple 2 top	18.87	19.74	0.87	15087	0	19.74	67713
Avulsion/Base LIRB4	18.41	18.87	0.46	0	460	18.87	52626
Purple 1 top	18.18	18.41	0.23	3988	0	18.41	52166
Avulsion/Base LIRB3	17.89	18.18	0.29	0	290	18.18	48178
LIRB2 top	16.56	17.89	1.33	23064	0	17.65	47888
Avulsion/Base LIRB2	15.84	16.56	0.72	0	720	16.56	24824
LIRB 1 top	14.45	15.84	1.39	24104	0	15.84	24104
LIRB 1 base						14.45	0

Table S4. Regression statistics for natural log of *Sifrhippus* M/1 area on *Coryphodon* $\delta^{18}O_E$ values. P-values significant with 95% confidence are shown in bold.

Start Level	n Bins	R^2	*P*	DW	DW L	DW U	SW $\delta^{18}O$	SW M/1
6 Meter Bins								
8	6	0.77	**0.022**	2.43	0.61	1.40	0.59	0.92
9	9	0.60	**0.014**	1.90	0.82	1.32	0.82	0.56
10	9	0.71	**0.005**	1.61	0.82	1.32	0.67	0.25
11	9	0.67	**0.007**	1.82	0.82	1.32	0.52	0.19
12	9	0.67	**0.007**	1.63	0.82	1.32	0.72	0.41
13	8	0.75	**0.005**	**1.26**	0.76	1.33	0.52	0.54
means	8.3	0.70	**0.010**					
5 Meter Bins								
8	9	0.74	**0.003**	1.36	0.82	1.32	1.00	0.52
9	8	0.51	**0.046**	2.03	0.76	1.33	0.95	0.72
10	9	0.53	**0.027**	1.76	0.82	1.32	0.90	0.46
11	8	0.69	**0.010**	1.47	0.76	1.33	0.25	0.31
12	8	0.77	**0.004**	2.05	0.76	1.33	0.80	0.28
means	8.4	0.65	**0.018**					
4 Meter Bins								
9	8	0.59	**0.026**	2.40	0.76	1.33	0.46	0.41
10	9	0.60	**0.015**	**1.24**	0.82	1.32	0.27	0.61
11	10	0.58	**0.011**	**1.09**	0.88	1.32	0.68	0.56
12	9	0.72	**0.028**	2.51	0.82	1.32	0.38	0.70
means	9.0	0.62	**0.020**					

Abbreviations: n, number of bins; R^2, coefficient of determination; *p*, probability of random correlation; DWL, DW, Durbin Watson statistic; Durbin-Watson lower critical value; DWL, Durbin-Watson upper critical value; SW, Shapiro-Wilk statistic.

Table S5. Regression statistics for natural log of *Sifrhippus* M/1 area on *Sifrhippus* $\delta^{18}O_E$ values. P-values significant with 95% confidence shown in bold.

6 Meter Bins								
Start Level	**n Bins**	**R^2**	***p***	**DW**	**DW L**	**DW U**	**SW $\delta^{18}O$**	**SW M/1**
9	9	0.41	0.064	1.33	0.82	1.32	**0.04**	0.34
10	10	0.38	0.057	**1.16**	0.88	1.32	0.14	0.15
11	10	0.40	**0.049**	**1.21**	0.88	1.32	0.10	0.09
12	9	0.67	**0.007**	1.35	0.82	1.32	0.38	0.18
13	8	0.48	0.056	1.38	0.76	1.33	0.21	0.26
14	7	0.62	**0.035**	1.94	0.70	1.36	0.11	0.71
means	8.8	0.494	**0.045**					
5 Meter Bins								
10	11	0.39	0.057	1.51	0.93	1.32	0.23	**0.04**
11	10	0.45	**0.033**	**1.10**	0.88	1.32	0.21	0.16
12	9	0.38	0.075	**1.21**	0.82	1.32	**0.04**	**0.04**
13	10	0.69	**0.003**	1.59	0.88	1.32	0.29	0.29
14	9	0.35	0.096	1.53	0.82	1.32	0.56	0.33
means	9.8	0.453	0.053					
4 Meter Bins								
11	12	0.42	**0.022**	**1.11**	0.97	1.33	**0.04**	0.45
12	11	0.67	**0.002**	**1.05**	0.93	1.32	0.87	0.81
13	10	0.33	0.084	1.42	0.88	1.32	0.44	0.06
14	11	0.38	**0.042**	**1.08**	0.93	1.32	0.16	0.17
means	11.0	0.450	**0.038**					

Abbreviations as in Table S3

Table S6. Regression statistics for natural log of faunal (*Ectocion*, *Copecion*, *Sifrhippus*) $\delta^{13}C_E$ values on *Coryphodon* $\delta^{18}O$ values. P-values significant with 95% confidence shown in bold.

6 Meter Bins								
Start Level	**n Bins**	**R2**	***p***	**DW**	**DW L**	**DW U**	**SW δ18O**	**SW M/1**
-4	8	0.78	**0.004**	1.80	0.76	1.33	0.76	0.07
-3	9	0.51	**0.031**	2.08	0.82	1.32	0.72	0.10
-2	10	0.39	0.054	2.08	0.88	1.32	0.62	0.18
-1	10	0.46	**0.031**	2.20	0.88	1.32	0.38	0.13
0	9	0.48	**0.038**	2.31	0.82	1.32	0.62	0.20
1	8	0.56	**0.033**	2.26	0.76	1.33	0.69	0.14
means	9.0	0.529	**0.032**					
5 Meter Bins								
1	10	0.60	**0.008**	2.51	0.88	1.32	0.27	0.37
0	10	0.47	**0.028**	2.24	0.88	1.32	0.80	0.14
-1	10	0.45	**0.035**	2.10	0.88	1.32	0.79	0.10
-2	9	0.55	**0.022**	1.97	0.82	1.32	0.87	**0.04**
-3	10	0.46	**0.032**	1.57	0.88	1.32	0.82	**0.04**
means	9.8	0.506	**0.025**					
4 Meter Bins								
-2	11	0.47	**0.020**	1.79	0.93	1.32	0.25	0.59
-1	11	0.44	**0.026**	1.93	0.93	1.32	0.49	0.40
0	11	0.51	**0.014**	2.15	0.93	1.32	0.87	**0.04**
1	10	0.46	**0.031**	1.93	0.88	1.32	0.92	**0.05**
means	10.8	0.470	**0.023**					

Abbreviations as in Table S3

Table S7. List of PETM mammal species showing average estimated change in body mass from pre-PETM congeners (pre-CIE, *Copecion* biozone, Cf-3) to PETM (*Meniscotherium priscum* and "*Hyracotherium*" *sandrae* biozones), and PETM to post-PETM congeners (post-CIE, *Cardiolophus radinskyi* biozone, Wa-1) intervals. All estimates are based on first lower molar area, except for *Palaeanodon*, which is based on humeral radial measurements. Data for *Sifrhippus* from this study. See SOM text for caveats regarding some taxa.

Order	Family	PETM species	% change Pre-PETM to PETM	% change PETM to Post-PETM	Diet	Locomotor Behavior	Range Through?	Sources
Multituberculata	Ptilodontidae	*Ectypodus tardus*	0	0	Omnivore	A	R	(*1-4*)
Multituberculata	Ptilodontidae	*Parectypodus lunatus*	-	0	Omnivore	A	FA	(*1, 3, 4*)
Didelphimorphia	Didelphidae	*Mimoperadectes labrus*	0	0	Omnivore	S/A	R	(*1-5*)
Didelphimorphia	Didelphidae	*Peradectes protinnominatus*	0	0	Omnivore	S/A	R	(*1, 3-5*)
Didelphimorphia	Herpetotheriidae	*Peratherium innominatum*	0	0	Omnivore	S/A	R	(*1, 3, 4*)
Rodentia	Ischyromyidae	*Acritoparamys atwateri*	0	0	Herbivore	S	R	(*1-4*)
Rodentia	Ischyromyidae	*Microparamys hunterae*	-	0	Herbivore	S	FA	(*1, 6*)
Rodentia	Ischyromyidae	*Paramys annectens*	0	0	Herbivore	S	R	(*1, 6*)
Rodentia	Ischyromyidae	*Paramys copei*	0	0	Herbivore	S	R	(*1, 3, 4*)
Rodentia	Ischyromyidae	*Paramys taurus*	0	0	Herbivore	S	R	(*1, 2, 4*)
Rodentia	Ischyromyidae	*Reithroparamys* sp.	-	0	Herbivore	S?	FA?	(*1, 6*)
Cimolesta	Apatemyidae	*Apatemys* sp.	0	0	Insectivore	A	R	(*1, 3, 5*)
Taeniodonta	Stylinodontidae	*Ectoganus bighornensis*	-	-	Herbivore	T	R	(*1, 2*)
Tillodontia	Esthonychidae	*Azygonyx gunnelli*	-40	-	Herbivore	T/S	R	(*1, 2, 4, 7*)
Tillodontia	Esthonychidae	*Esthonyx spatularius*	-	0	Herbivore	T	FA	(*1, 2*)
Pantodonta	Coryphodontidae	*Coryphodon* sp.	-	0	Herbivore	T	R	(*1-5*)
Palaeanodonta	Metacheiromyidae	*Palaeanodon nievelti*	-58	0	Insectivore	T	R	(*2, 8, 9*)
Creodonta	Hyaenodontidae	*Acarictis ryani*	-	0	Carnivore	T	FA	(*1-3, 10*)
Creodonta	Hyaenodontidae	*Arfia junnei*	-	82	Carnivore	T	FA	(*1*)
Creodonta	Hyaenodontidae	*Prolimnocyon eerius*	-	35	Carnivore	S	FA	(*1, 2*)

Creodonta	Hyaenodontidae	*Prototomus deimos*	-	29	Carnivore	S/A?	FA	(*2, 10*)
Creodonta	Oxyaenidae	*Dipsalidictis platypus*	0	0	Carnivore	T	R	(*1, 2, 11*)
Creodonta	Oxyaenidae	*Palaeonictis wingi*	-65	65	Carnivore/ Omnivore	T	R	(*1, 12*)
Carnivoramorpha	Miacidae	*Miacis deutschi*	-	0	Carnivore	S/A?	FA	(*1, 3, 13*)
Carnivoramorpha	Miacidae	*Miacis rosei*	-	-	Carnivore	S/A?	FA	(*1, 14*)
Carnivoramorpha	Miacidae	*Miacis winkleri*	-	0	Carnivore	S/A?	FA	(*1, 2, 13*)
Carnivoramorpha	Miacidae	*Uintacyon gingerichi*	-49	94	Carnivore/ Omnivore	S/A	R	(*1, 12, 14*)
Carnivoramorpha	Miacidae	*Vassacyon bowni*	-	80	Carnivore	S/A	FA	(*1, 14*)
Carnivoramorpha	Viverravidae	*Didymictis leptomylus*	0	0	Carnivore	T	R	(*1, 2, 4*)
Carnivoramorpha	Viverravidae	*Viverravus politus*	0	0	Carnivore	T	R	(*1, 3, 15*)
Erinaceomorpha	Amphilemuridae	*Macrocranion junnei*	-	-	Insectivore	T/Sa	FA	(*1, 3, 4, 16*)
Soricomorpha	Nyctitheriidae	*Plagioctenodon savagei*	-	0	Insectivore	S?	FA	(*1, 3*)
Primates	Adapidae	*Cantius torresi*	-	14	Frugivore	A	FA	(*1, 2*)
Primates	Micromomyidae	*Tinimomys graybulliensis*	0	0	Omnivore/ Insectivore?	A?	R	(*1, 3, 5, 17*)
Primates	Microsyopidae	*Arctodontomys wilsoni*	-	25	Omnivore/ Insectivore?	A?	FA	(*1, 2*)
Primates	Microsyopidae	*Niptomomys doreenae*	0	0	Omnivore/ Insectivore?	A?	R	(*1, 4*)
Primates	Microsyopidae	*Niptomomys favorum*	-	-	Omnivore/ Insectivore?	A?	R	(*1, 3, 6*)
Primates	Omomyidae	*Teilhardina brandti*	-	0	Omnivore/ Insectivore	A	FA	(*1, 18*)
Primates	Paromomyidae	*Phenacolemur praecox*	0	0	Frugivore/ Exudate-feeder	A	R	(*1, 2, 4*)
Condylarthra	Apheliscidae	*Haplomylus zalmouti*	-71	97	Herbivore	C/Sa	R	(*1, 6*)
Condylarthra	Arctocyonidae	*Chriacus badgleyi*	-55	62	Omnivore	S/A	R	(*1, 2*)
Condylarthra	Arctocyonidae	*Princetonia yalensis*	0	-	Omnivore?	T/S	R	(*1-3*)
Condylarthra	Arctocyonidae	*Thryptacodon barae*	-39	35	Omnivore	S/A?	R	(*1, 2, 5*)
Condylarthra	Hyopsodontidae	*Hyopsodus loomisi*	-46	16	Herbivore	T?	R	(*1, 2, 19*)
Condylarthra	Phenacodontidae	*Copecion davisi*	-46	85	Herbivore	T	R	(*1, 2*)
Condylarthra	Phenacodontidae	*Ectocion parvus*	-48	91	Herbivore	T	R	(*1, 2*)
Condylarthra	Phenacodontidae	*Phenacodus intermedius*	0	0	Herbivore	T	R	(*1-3, 20*)
Condylarthra	Phenacodontidae	*Phenacodus vortmani*	0	0	Herbivore	T	R	(*1-3, 6, 20*)
Mesonychia	Mesonychidae	*Dissacus praenuntius*	0	0	Carnivore	T/C	R	(*1-3*)
Mesonychia	Mesonychidae	*Pachyaena ossifraga*	-	0	Carnivore	T/C	FA	(*1, 4*)

Artiodactyla	Dichobunidae	*Diacodexis ilicis*	-	10	Herbivore	T/C	FA	(*1, 2, 19*)
Perissodactyla	Equidae	*Sifrhippus sandrae*	-	76	Herbivore	T/C	FA	(*1, 2, 4, 21*)
Total species (for which body size approximations can be made)			29	45				
Total genera (for which body size approximations can be made)			26	40				
Paleocene genera with smaller PETM congeners			10					
PETM genera with smaller post-PETM congeners				16				
Percent Paleocene genera with smaller PETM congeners			38					
Percent PETM genera with smaller post-PETM congeners				40				

Abbreviations and symbols

- , species is either not present or is too poorly represented for estimate.

Locomotor behavior (Lcmtr Bhvr) Column**:** A, Arboreal; C, Cursorial; S, Scansorial; Sa, Saltatorial; T, Terrestrial.

Range Through? Column: Range through: R, range through; FA, first appearance.

Table S8. First molar (M/1) measurements for the equid *Sifrhippus* used to estimate body size changes.

Specimen UF #	Specimen Field #	Locality	Biozone	Genus	Species	Element	Length (mm)	Width (mm)	Ln (L x W)	Mass (Kg)	Meter Level
259925	CAB09-0599	v06153	Wa-1	*Sifrhippus*	*grangeri*	M/1	6.88	4.72	3.48	7.47	75.32
254107	CAB09-0601	v06153	Wa-1	*Sifrhippus*	*grangeri*	M/1	6.85	4.73	3.48	7.44	75.32
259934	CAB09-1133	v08002	Wa-1	*Sifrhippus*	*grangeri*	M/1	7.86	5.48	3.76	11.45	75.32
253970	CAB08-1036	v08179	Wa-1	*Sifrhippus*	*grangeri*	M/1	7.05	4.89	3.54	8.18	73.37
259931	CAB09-0867	v08179	Wa-1	*Sifrhippus*	*grangeri*	M/1	6.56	4.86	3.46	7.26	73.37
259932	CAB09-0875	v08179	Wa-1	*Sifrhippus*	*grangeri*	M/1	7.27	4.64	3.52	7.91	73.37
252291	CAB06-671	v06131	Wa-1	*Sifrhippus*	*grangeri*	M/1	6.90	4.61	3.46	7.24	72.96
253865	CAB08-877	v08178	Wa-1	*Sifrhippus*	*grangeri*	M/1	6.99	4.77	3.51	7.77	72.52
259929	CAB09-0829	v08178	Wa-1	*Sifrhippus*	*grangeri*	M/1	6.86	4.85	3.50	7.75	72.52
259937	CAB10-0314	v10035	Wa-1	*Sifrhippus*	*grangeri*	M/1	7.53	5.28	3.68	10.14	69.97
254006	CAB08-1072	v07056	Wa-1	*Sifrhippus*	*grangeri*	M/1	7.30	4.96	3.59	8.81	68.57
254103	CAB08-1119	v08114	Wa-1	*Sifrhippus*	*grangeri*	M/1	7.53	5.20	3.67	9.91	62.77
259933	CAB09-0977	v09189	Wa-1	*Sifrhippus*	*sandrae*	M/1	7.25	5.06	3.60	8.98	61.95
253280	CAB08-288	v08075	Wa-1	*Sifrhippus*	*grangeri*	M/1	7.34	5.15	3.63	9.40	47.50
251424	CAB05-584	v05037	Wa-0?	*Sifrhippus*	*grangeri*	M/1	7.15	4.78	3.53	8.07	45.10
251461	CAB06-010	v06010	Wa-0	*Sifrhippus*	*sandrae*	M/1	6.49	4.47	3.37	6.30	44.20
250499	CAB05-150-02	v05009	Wa-0	*Sifrhippus*	*sandrae*	M/1	6.36	3.92	3.22	5.01	40.90
251778	CAB06-248	v06057	Wa-0	*Sifrhippus*	*sandrae*	M/1	5.95	3.98	3.16	4.63	40.90
259921	CAB09-0367	v09110	Wa-0	*Sifrhippus*	*sandrae*	M/1	6.46	4.23	3.31	5.75	40.90
259922	CAB09-0369	v09110	Wa-0	*Sifrhippus*	*sandrae*	M/1	6.14	4.20	3.25	5.27	40.90
259923	CAB09-0451	v09130	Wa-0	*Sifrhippus*	*sandrae*	M/1	6.05	3.87	3.15	4.55	40.90
259924	CAB09-0494	v09123	Wa-0	*Sifrhippus*	*sandrae*	M/1	6.20	3.58	3.10	4.20	40.90
259928	CAB09-0734	v08154	Wa-0	*Sifrhippus*	*sandrae*	M/1	6.26	4.22	3.27	5.46	40.00
259935	CAB10-0102	v09110	Wa-0	*Sifrhippus*	*sandrae*	M/1	6.46	4.31	3.33	5.92	40.00
259938	CAB10-0434	v10060	Wa-0	*Sifrhippus*	*sandrae*	M/1	6.05	4.01	3.19	4.80	36.25
259939	CAB10-0443	v10060	Wa-0	*Sifrhippus*	*sandrae*	M/1	6.63	4.16	3.32	5.83	36.25
259919	CAB09-0199	v09050	Wa-0	*Sifrhippus*	*sandrae*	M/1	6.16	3.99	3.20	4.90	34.98
253060	CAB08-067	v08011	Wa-0	*Sifrhippus*	*sandrae*	M/1	6.58	4.44	3.37	6.36	32.07
253061	CAB08-068	v08011	Wa-0	*Sifrhippus*	*sandrae*	M/1	6.06	4.05	3.20	4.89	32.07
253062	CAB08-069	v08011	Wa-0	*Sifrhippus*	*sandrae*	M/1	5.99	3.94	3.16	4.61	32.07
253063	CAB08-070	v08011	Wa-0	*Sifrhippus*	*sandrae*	M/1	6.33	4.20	3.28	5.52	32.07
259927	CAB09-0672	v09158	Wa-0	*Sifrhippus*	*sandrae*	M/1	6.44	4.03	3.26	5.32	24.85
253508	CAB08-516	v08106	Wa-0	*Sifrhippus*	*sandrae*	M/1	6.90	4.22	3.37	6.33	24.35

250055	CAB04-512	v04148	Wa-0	*Sifrhippus*	*sandrae*	M/1	6.84	4.32	3.39	6.47	23.66
259936	CAB10-0259	v05108	Wa-0	*Sifrhippus*	*sandrae*	M/1	6.25	4.17	3.26	5.35	23.11
249832	CAB04-392	v04105	Wa-0	*Sifrhippus*	*sandrae*	M/1	6.70	4.33	3.37	6.30	20.75
259920	CAB09-0247	v09063	Wa-0	*Sifrhippus*	*sandrae*	M/1	6.69	4.26	3.35	6.13	17.65
254902	CAB09-0785	v09174	Wa-0	*Sifrhippus*	*sandrae*	M/1	6.95	4.53	3.45	7.13	17.65
250233	CAB05-030-31	v05006	Wa-0	*Sifrhippus*	*sandrae*	M/1	6.62	4.84	3.47	7.32	17.02
250234	CAB05-030-32	v05006	Wa-0	*Sifrhippus*	*sandrae*	M/1	6.60	4.48	3.39	6.48	17.02
250203	CAB05-030-49	v05006	Wa-0	*Sifrhippus*	*sandrae*	M/1	6.76	4.5	3.42	6.77	17.02
251562	CAB06-078-2	v05006	Wa-0	*Sifrhippus*	*sandrae*	M/1	6.78	4.47	3.41	6.73	17.02
251570	CAB06-079	v05006	Wa-0	*Sifrhippus*	*sandrae*	M/1	7.07	4.74	3.51	7.83	17.02
251517	CAB06-054-02	v06014	Wa-0	*Sifrhippus*	*sandrae*	M/1	6.83	4.57	3.44	7.03	14.45

Table S9. Fossil teeth sampled for stable isotopes.

USNM #	UF #	Sample #	Field #	Locality #	Biozone	Genus	Species	$\delta^{13}C$	$\delta^{18}O$	Meter Level	Element Sampled
	250459	SB1-01	CAB05-587	v05108	Wa-0	*Ectocion*	*parvus*	-14.5	22.7	23.11	R M3/
	250759	SB1-02	CAB05-264	v05067	Wa-0	*Ectocion*	*parvus*	-13.9	24.9	17.65	L M/1
	249223	SB1-04	CAB04-022	v04005	Cf-3	*Ectocion*	*osbornianus*	-7.4	23.2	2.29	L M/2
	249291	SB1-09	CAB04-087	v04017	Cf-3	*Ectocion*	*osbornianus*	-10.4	22.3	2.14	L P4/
	249297	SB1-10	CAB04-093	v04017	Cf-3	*Ectocion*	*osbornianus*	-11.6	20.7	2.14	R M/3
	249331	SB1-11	CAB04-121	v04027	Cf-3	*Ectocion*	*osbornianus*	-11.4	21.4	2.82	L M/1
	249358	SB1-13	CAB04-142-A	v04037	Cf-3	*Copecion*	*brachypternus*	-9.8	22.2	2.38	R M1/
	249358	SB1-14	CAB04-142-B	v04037	Cf-3	*Copecion*	*brachypternus*	-10.7	22.1	2.38	R M/1
	249365	SB1-15	CAB04-148	v04040	Cf-3	*Ectocion*	*osbornianus*	-12.0	21.2	1.00	R M/3
	249376	SB1-16	CAB04-155	v04041	Cf-3	*Ectocion* or *Copecion*	*osbornianus* or *brachypternus*	-11.9	20.4	2.79	Mx/ frag
	249379	SB1-17	CAB04-158-1	v04042	Cf-3	*Ectocion* or *Copecion*	*osbornianus* or *brachypternus*	-10.2	21.8	2.79	L P4/
	249661	SB1-20	3	v04105	Wa-0	*Ectocion*	*parvus*	-13.7	23.2	20.75	R M3/
	249811	SB1-21	CAB04-371	v04105	Wa-0	*Copecion*	*davisi*	-14.1	23.2	20.75	R M/1 or M/2
	249816	SB1-22	CAB04-376	v04105	Wa-0	*Ectocion*	*parvus*	-14.3	25.0	20.75	R M2/
	249817	SB1-23	CAB04-377	v04105	Wa-0	*Copecion*	*davisi*	-14.1	23.8	20.75	L M2/
	249819	SB1-24	CAB04-379	v04105	Wa-0	*Copecion*	*davisi*	-14.8	23.6	20.75	R M1/
	249822	SB1-25	CAB04-382	v04105	Wa-0	*Ectocion*	*parvus*	-14.8	21.0	20.75	L M/1
	249824	SB1-26	CAB04-384	v04105	Wa-0	*Ectocion*	*parvus*	-14.6	22.7	20.75	L M/1
	249833	SB1-27	CAB04-393	v04105	Wa-0	*Copecion*	*davisi*	-14.9	20.9	20.75	R M/1
	249856	SB1-29	CAB04-408	v04105	Wa-0	*Ectocion*	*parvus*	-13.1	21.7	20.75	R P/3
	249858	SB1-30	CAB04-410	v04105	Wa-0	*Ectocion*	*parvus*	-16.6	22.2	20.75	L M/1
	249859	SB1-31	CAB04-411	v04105	Wa-0	*Copecion*	*davisi*	-14.5	23.1	20.75	R M/1
	249861	SB1-32	CAB04-413	v04105	Wa-0	*Copecion*	*davisi*	-14.8	22.0	20.75	L M2/
	251619	SB1-33	CAB06-123	v04105	Wa-0	*Copecion*	*davisi*	-14.2	22.7	20.75	L P/4
	251620	SB1-34	CAB06-124	v04105	Wa-0	*Ectocion*	*parvus*	-14.3	24.3	20.75	R M/2
	252519	SB1-35	CAB07-572	v04105	Wa-0	*Copecion*	*davisi*	-14.2	22.9	20.75	R M/2
	250876	SB1-38	CAB05-322	v05052	Wa-0	*Ectocion*	*parvus*	-14.6	21.4	22.57	R M2/
	251137	SB1-39	CAB05-450	v05127	Wa-0	*Sifrhippus*	*sandrae*	-14.6	25.1	15.24	M/3
	252100	SB1-40	CAB06-486	v06126	Wa-0	*Copecion*	*brachypternus*	-15.2	22.8	45.91	L M/2
	250113	SB1-42	CAB04-534-1	v04162	Wa-0?	*Coryphodon*	*eocaenus*	-15.5	21.8	19.91	enamel frag.
	249351	SB1-43	CAB04-136	v04034	Wa-0	*Coryphodon*	*eocaenus*	-15.4	22.6	19.80	enamel frag.

	250169	SB2-01	CAB05-009	(L)nw0350	Wa-1	*Ectocion*	*osbornianus*	-12.5	20.9	47.19	L M/2
	252657	SB2-02	CAB07-257	v07055	Wa-1	*Ectocion*	*osbornianus*	-11.9	21.4	67.22	R P4/
	252927	SB2-03	CAB07-490	v07115	Wa-1?	*Ectocion*	*osbornianus*	-10.5	24.0	62.77	L P4/
	252505	SB2-04	CAB07-127	v07034	Wa-1?	*Ectocion*	*osbornianus*	-12.9	21.7	66.54	L M/2
	252946	SB2-05	CAB07-509	v07116	Wa-1	*Ectocion*	*osbornianus*	-13.5	19.9	66.83	L M3/
	252636	SB2-06	CAB07-236	v07055	Wa-1	*Ectocion*	*osbornianus*	-13.6	18.3	67.22	L P4/ frag.
	252500	SB2-07	CAB07-122	v07033	Wa-1	*Copecion*	*brachypternus*	-12.4	21.6	66.78	M2/ part
	252541	SB2-09	CAB07-143	v07037	Wa-1	*Copecion*	*brachypternus*	-13.0	24.4	46.50	L M/2
	252239	SB2-10	CAB06-623	v06129	Wa-1	*Copecion*	*brachypternus*	-13.0	21.3	69.97	L M/2
	250366	SB2-12	CAB05-065	v05109	Wa-0	*Ectocion*	*parvus*	-12.9	25.3	24.85	R M2/
	251374	SB2-13	CAB05-559	v05128	Wa-0	*Ectocion*	*parvus*	-13.8	24.2	16.40	R M2/
488280		SB2-14	NW03-085a	(L)nw0321	Wa-0	*Ectocion*	*parvus*	-16.3	20.6	29.24	R M3/
	250779	SB2-15	CAB05-273	v05029	Wa-0	*Ectocion*	*parvus*	-15.8	21.2	17.65	R M1/
	250372	SB2-16	CAB05-068	v05005	Wa-0	*Ectocion*	*parvus*	-16.0	21.4	16.42	L P/4 part
	251380	SB2-17	CAB05-565	v05128	Wa-0	*Copecion*	*davisi*	-14.3	24.4	16.40	L P/4
	250339	SB2-18	CAB05-051	v05001	Wa-0	*Copecion*	*davisi*	-13.7	22.4	14.45	R P/4
	251418	SB2-19	CAB05-582	v05123	Wa-1	*Copecion*	*brachypternus* or *davisi*	-13.3	23.7	46.43	L M/2
	251559	SB2-22	CAB06-076	v06016	Wa-M?	*Coryphodon*	*proterus*	-15.6	21.3	11.75	R molar trigonid
	252244	SB2-24	CAB06-628-1	v06132	Wa-1	*Coryphodon*	*eocaenus*	-12.5	21.2	60.92	incisor
	252223	SB3-01	CAB06-607	v06118	Wa-0	*Coryphodon*	*eocaenus*	-15.8	23.6	24.85	enamel frag.
	252387	SB3-02	CAB07-051	v07010	Wa-1	*Coryphodon*	*eocaenus*	-13.9	22.7	60.01	enamel frag.
	252558	SB3-04	CAB07-161	v07044	Wa-0	*Coryphodon*	*eocaenus*	-16.1	23.3	40.90	enamel frag.
	250987	SB3-06	CAB05-376-4	v05053	Wa-0	*Coryphodon*	*eocaenus*	-15.3	22.7	22.17	enamel frag.
	252644	SB3-08	CAB07-244	v07055	Wa-1	*Coryphodon*	*eocaenus*	-14.6	20.8	67.22	enamel frag.
	252521	SB3-09	CAB07-402	v07087	Wa-0	*Coryphodon*	*eocaenus*	-17.6	22.5	26.46	enamel frag.
	251208	SB3-10	CAB05-479-1	esc05029	Wa-0	*Coryphodon*	*eocaenus*	-15.2	22.8	18.83	enamel frag.
	252502	SB3-11	CAB07-124	v07034	Wa-1?	*Coryphodon*	*eocaenus*	-14.4	21.7	66.54	enamel frag.
	252501	SB3-12	CAB07-123	v07033	Wa-1	*Coryphodon*	*eocaenus*	-13.7	21.9	66.78	enamel frag.
	252546	SB3-13	CAB07-148	v07039	Wa-1	*Coryphodon*	*eocaenus*	-15.5	21.1	46.50	enamel frag.
	252645	SB3-14	CAB07-245	v07055	Wa-1	*Coryphodon*	*eocaenus*	-13.6	21.7	67.22	enamel frag.
	251609	SB3-15	CAB06-114	v06022	Wa-0	*Coryphodon*	*eocaenus*	-15.3	20.7	14.45	enamel frag.
	251455	SB3-16	CAB06-004	v06001	Wa-0	*Coryphodon*	*eocaenus*	-14.9	20.5	46.84	enamel frag.
	251893	SB3-17	CAB06-326	v06068	Wa-0	*Coryphodon*	*eocaenus*	-15.0	24.2	45.10	enamel frag.

	251473	SB3-18	CAB06-021	v06003	Wa-0	*Coryphodon*	*eocaenus*	-14.9	20.3	47.64	Px/
	252339	SB3-19	CAB06-717	v06147	Wa-0	*Coryphodon*	*eocaenus*	-12.6	20.7	73.37	enamel frag.
	251559	SB3-20	CAB06-076f	v06016	Wa-M?	*Coryphodon*	*proterus*	-15.0	21.6	11.75	L M/3 trigonid
	252146	SB3-21	CAB06-530	v06118	Wa-0	*Coryphodon*	*eocaenus*	-16.7	22.7	24.85	enamel frag.
	251153	SB3-22	CAB05-459	akh0509	Wa-0	*Coryphodon*	*eocaenus*	-17.2	21.5	45.87	enamel frag.
	252101	SB3-23	CAB06-487	v06126	Wa-0	*Coryphodon*	*eocaenus*	-15.9	23.4	45.91	enamel frag.
	251362	SB3-24	CAB05-552-1	akh0500 9	Wa-0	*Coryphodon*	*eocaenus*	-16.1	20.9	45.87	enamel frag.
	251544	SB3-25	CAB06-064	v06022	Wa-0	*Coryphodon*	*eocaenus*	-15.9	22.1	14.45	enamel frag.
488301		SB3-26	NW03-051a	(L)nw03 21	Wa-0	*Coryphodon*	*eocaenus*	-16.2	24.2	29.24	enamel frag.
	251740	SB3-27	CAB06-226	v06054	Wa-0	*Coryphodon*	*eocaenus*	-15.8	23.1	40.90	Mx frag
	252398	SB3-28	CAB07-062	v07015	Wa-1	*Coryphodon*	*eocaenus*	-17.6	21.8	43.14	enamel frag.
	250965	SB3-29	CAB05-364	v05073	Cf-3	*Ectocion*	*osbornianus*	-10.4	21.3	-11.46	m/3
	251559	SB3-30	CAB06-076a	v06016	Wa-M?	*Coryphodon*	*proterus*	-14.2	21.3	11.75	L M2/
	251559	SB3-31	CAB06-076b	v06016	Wa-M?	*Coryphodon*	*proterus*	-15.1	21.2	11.75	L P3/
	251559	SB3-32	CAB06-076c	v06016	Wa-M?	*Coryphodon*	*proterus*	-15.1	21.4	11.75	L P4/
	252929	SB4-04	CAB07-492	v07115	Wa-1?	*Coryphodon*	*eocaenus*	-12.4	21.7	62.77	?
	252672	SB4-05	CAB07-272	v07055	Wa-1	*Coryphodon*	*eocaenus*	-13.1	20.5	67.22	enamel frag.
	252260	SB5-01	CAB06-641	v06134	Wa-0	*Sifrhippus*	*sandrae*	-16.2	22.2	19.27	L M/3
	250934	SB5-02	CAB05-349	v05113	Wa-0	*Sifrhippus*	*sandrae*	-13.1	24.8	21.02	L M3/
	251446	SB5-03	CAB06-002-15	v06014	Wa-0	*Sifrhippus*	*sandrae*	-14.9	24.1	14.45	L M3/
	252298	SB5-04	CAB06-678	v06146	Wa-1	*Sifrhippus*	*grangeri*	-12.6	20.0	69.97	L dent M/3
	250210	SB5-06	CAB05-030-005	v05006	Wa-0	*Sifrhippus*	*sandrae*	-14.5	25.1	17.02	L M3/
	250197	SB5-07	CAB05-030-001	v05006	Wa-0	*Sifrhippus*	*sandrae*	-14.8	24.3	17.02	L M3/
	250207	SB5-08	CAB05-030-002	v05006	Wa-0	*Sifrhippus*	*sandrae*	-14.7	25.1	17.02	R M3/
	250910	SB5-09	CAB05-337	v05030	Wa-0	*Sifrhippus*	*sandrae*	-12.5	26.0	24.12	L M2/
	250211	SB5-10	CAB05-030-006	v05006	Wa-0	*Sifrhippus*	*sandrae*	-15.0	24.3	17.02	L M3/
	250212	SB5-12	CAB05-030-007	v05006	Wa-0	*Sifrhippus*	*sandrae*	-15.2	23.0	17.02	L M3/
	250238	SB5-13	CAB05-030-037	v05006	Wa-0	*Sifrhippus*	*sandrae*	-14.8	23.8	17.02	L M/3
	249854	SB5-14	CAB04-406	v04105	Wa-0	*Sifrhippus*	*sandrae*	-15.9	22.5	20.75	R M/3
	252953	SB5-15	CAB07-517	v07031	Wa-1	*Sifrhippus*	*grangeri*	-11.3	21.7	68.51	R M/3
	250209	SB5-16	CAB05-030-004	v05006	Wa-0	*Sifrhippus*	*sandrae*	-14.4	24.4	17.02	R M3/
	250237	SB5-17	CAB05-030-036	v05006	Wa-0	*Sifrhippus*	*sandrae*	-13.2	23.9	17.02	R M/3
	251360	SB5-18	CAB05-551-1	v05122	Wa-1	*Sifrhippus*	*sandrae*	-14.1	24.7	45.87	R M3/
	252156	SB5-19	CAB06-540	v06119	Wa-0	*Sifrhippus*	*sandrae*	-13.8	23.9	18.47	L M3/
	251445	SB5-20	CAB06-002-14	v06014	Wa-0	*Sifrhippus*	*sandrae*	-14.6	24.0	14.45	L M3/

	251928	SB5-21	CAB06-344	v06084	Wa-0	*Sifrhippus*	*sandrae*	-17.0	21.4	40.90	L M3/
	252697	SB5-22	CAB07-287	v07056	Wa-1	*Sifrhippus*	*grangeri*	-11.9	20.2	68.57	L M3/
	252234	SB5-23	CAB06-618	v06129	Wa-1	*Sifrhippus*	*grangeri*	-12.9	20.8	69.97	R M/3
	252040	SB5-24	CAB06-435	v06105	Wa-1	*Sifrhippus*	*grangeri*	-16.1	22.3	46.45	L M3/
	251658	SB5-25	CAB06-157	v06039	Wa-0	*Sifrhippus*	*sandrae*	-14.8	25.0	40.90	L M/3
	251175	SB5-26	CAB05-466	v05118	Wa-0	*Sifrhippus*	*sandrae*	-14.9	22.8	25.19	M/3
	252007	SB5-27	CAB06-402	v06109	Wa-0?	*Sifrhippus*	*sandrae*	-14.9	22.8	40.90	R M3/
488295		SB5-28	NW03-038	(L)nw03 18	Wa-0	*Sifrhippus*	*sandrae*	-13.7	24.7	31.40	M/2
	252242	SB5-29	CAB06-626	v06130	Wa-1	*Sifrhippus*	*grangeri*	-11.7	20.5	71.42	L M/3
	252431	SB5-30	CAB07-037	v07008	Wa-1	*Sifrhippus*	*grangeri*	-11.5	19.6	48.10	R M3/
	252730	SB5-31	CAB07-320	v07061	Wa-1	*Sifrhippus*	*grangeri*	-12.0	17.6	65.67	R M/3
	251440	SB5-32	CAB06-002-09	v06014	Wa-0	*Sifrhippus*	*sandrae*	-15.2	25.0	14.45	L M/3
	252639	SB5-33	CAB07-239	v07055	Wa-1	*Sifrhippus*	*grangeri*	-11.1	20.7	67.22	L M/3
	251713	SB5-34	CAB06-207	v06046	Wa-0	*Sifrhippus*	*sandrae*	-15.8	22.7	14.45	L M3/
	252357	SB5-36	CAB06-735	v06134	Wa-0	*Sifrhippus*	*sandrae*	-15.4	23.0	19.27	L M3/
	250208	SB5-37	CAB05-030-003	v05006	Wa-0	*Sifrhippus*	*sandrae*	-14.9	21.8	17.02	R M3/
493918		SB5-38	NW03-046	(L)nw03 21	Wa-0	*Sifrhippus*	*sandrae*	-14.3	21.4	29.24	R M/3
	251432	SB5-39	CAB06-002-01	v06014	Wa-0	*Sifrhippus*	*sandrae*	-14.9	24.7	14.45	R M/3
	250963	SB8-01	CAB05-362	V05076	cf-3	*Coryphodon*	*proterus*	-13.2	20.5	1.46	R C1/
	250890	SB8-26	CAB05-328	v05056	Cf-3	*Ectocion*	*osbornianus*	-9.8	22.5	5.38	L M/3
	250891	SB8-28	CAB05-329	v05056	Cf-3	*Ectocion*	*osbornianus*	-7.0	25.3	5.38	LM3/
	253630	SB8-30	CAB08-639	v04004	Cf-3	*Ectocion*	*osbornianus*	-9.7	23.5	2.82	L P4/
	250080	SB8-39	CAB04-549	v04005	Cf-3	*Ectocion*	*osbornianus*	-10.4	20.1	2.29	M3/
	253628	SB8-44	CAB08-637	v04004	Cf-3	*Ectocion*	*osbornianus*	-9.7	17.5	2.82	RM/1
	250808	SB8-45	CAB05-285	v05031	Cf-3	*Ectocion*	*osbornianus*	-10.0	24.5	3.98	LM1/
	250825	SB8-48	CAB05-297	v05063	Cf-3	*Ectocion*	*osbornianus*	-9.8	26.0	5.99	LP/3
	252451	SB8-49	CAB07-072	v07018	Cf-3	*Ectocion*	*osbornianus*	-7.1	27.7	4.98	M3/
	249299	SB8-50	CAB04-095	v04017	Cf-3	*Ectocion*	*osbornianus*	-10.7	22.9	2.14	LP/3
	249298	SB8-51	CAB04-094	v04017	Cf-3	*Ectocion*	*osbornianus*	-7.8	23.3	2.14	RP3/
	253641	SB9-01	CAB08-650	v08140	Wa-0	*Sifrhippus*	*sandrae*	-14.8	24.8	43.35	RM3/
	253382	SB9-02	CAB08-390	v08091	Wa-0	*Sifrhippus*	*sandrae*	-14.1	23.4	36.48	LM3/
	253319	SB9-04	CAB08-327	v08077	Wa-0	*Sifrhippus*	*sandrae*	-12.6	26.4	40.90	LM/3
	254047	SB9-05	CAB08-967	v08185	Wa-0	*Sifrhippus*	*sandrae*	-15.8	21.4	20.72	RM3/
	253406	SB9-06	CAB08-414	v08077	Wa-0	*Sifrhippus*	*sandrae*	-12.2	26.7	40.90	RM1/ broken
	253058	SB9-07	CAB08-065	v08016	Wa-0	*Sifrhippus*	*sandrae*	-15.1	23.0	31.66	LP4/

252554	SB9-08	CAB07-157	v07044	Wa-0	*Sifrhippus*	*sandrae*	-13.2	22.3	40.90	LP/3
253727	SB9-09	CAB08-739	v08161	Wa-0	*Sifrhippus*	*sandrae*	-13.2	24.4	45.10	LM2/
252748	SB9-10	CAB07-333	v07066	Wa-0?	*Sifrhippus*	*sandrae*	-12.5	30.5	40.90	LP4/
253987	SB9-12	CAB08-1053	v08191	Wa-0	*Sifrhippus*	*sandrae*	-14.6	24.6	40.90	RP3/
253475	SB9-13	CAB08-483	v08112	Wa-0	*Sifrhippus*	*sandrae*	-12.0	27.1	45.10	LM2/
253371	SB9-14	CAB08-379	v08087b	Wa-0	*Sifrhippus*	*sandrae*	-15.2	22.8	45.10	RP4/
253509	SB9-15	CAB08-517	v08106	Wa-0	*Sifrhippus*	*sandrae*	-16.8	22.0	24.35	M/2
252772	SB9-16	CAB07-355	v07008	Wa-1	*Sifrhippus*	*grangeri*	-12.3	23.8	48.10	RM1/
252545	SB9-17	CAB07-147	v07039	Wa-1	*Sifrhippus*	*grangeri*	-12.6	25.8	46.50	LM/1 or M/2 frag.
253272	SB9-18	CAB08-280	v08070	Wa-1	*Sifrhippus*	*sandrae*	-13.3	25.2	40.90	
253988	SB9-19	CAB08-1054	v08191	Wa-0	*Sifrhippus*	*sandrae*	-14.4	25.0	40.90	RM2/
253558	SB9-21	CAB08-566	v08114	Wa-1	*Sifrhippus*	*grangeri*	-10.2	21.2	62.77	LM3/
253768	SB9-22	CAB08-779	v08173	Wa-0	*Sifrhippus*	*sandrae*	-15.5	25.0	40.90	RM1/
253064	SB9-23	CAB08-071	v08011	Wa-0	*Sifrhippus*	*sandrae*	-13.2	25.6	32.07	L M/2
253556	SB9-24	CAB08-564	v08114	Wa-1	*Sifrhippus*	*grangeri*	-12.2	20.1	62.77	RM/3 broken
253561	SB9-25	CAB08-569	v08114	Wa-1	*Sifrhippus*	*grangeri*	-11.5	23.8	62.77	RM3/
254092	SB9-26	CAB08-1108	v08192	Wa-1	*Sifrhippus*	*grangeri*	-12.4	28.0	46.50	LM/2
253250	SB9-27	CAB08-258	v08059	Wa-0	*Sifrhippus*	*sandrae*	-15.4	21.6	23.85	RM3/
254089	SB9-28	CAB08-1105	v08192	Wa-1	*Sifrhippus*	*grangeri*	-12.6	22.7	46.50	M/3
253063	SB9-29	CAB08-070	v08011	Wa-0	*Sifrhippus*	*sandrae*	-13.8	26.7	32.07	M/2

Pre-CIE (Cf-3) occurrences of taxa otherwise known only from the PETM, presumed to be contaminants based on excursion-level $\delta^{13}C$ values

	SB1-41	CAB07-104	v07027	Cf-3	*Ectocion*	*parvus*	-15.2	22.6	-3.25	R M/1 or M/2
	SB1-37	CAB04-544	v04167	Cf-3	*Copecion*	*davisi*	-14.3	22.6		L M/1 or M/2
	SB1-18	CAB04-190	v04049	Cf-3	*Copecion*	*davisi*	-13.9	23.6		L P/4
	SB1-12	CAB04-130	v04031	Cf-3	*Ectocion*	*parvus*	-13.9	23.7		L M1/
	SB1-05	CAB04-028	v04006	Cf-3	*Ectocion*	*parvus*	-13.1	25.4	2.29	R P4/
	SB8-27	CAB08-645	v08151	Cf-3	*Copecion*	sp.	-13.0	24.4	5.68	R M/1 or M/2
246800	SB4-28	CAB04-076	v04014	Cf-3	*Copecion*	*davisi*	-12.4	26.3	2.12	R M/2